

Posterior-based proposals for speeding up Markov chain Monte Carlo

C. M. Pooley^{1,2}, S. C. Bishop³, A. Doeschl-Wilson¹ and G. Marion²

1 The Roslin Institute, The University of Edinburgh, Midlothian, EH25 9RG, UK.

2 Biomathematics and Statistics Scotland, James Clerk Maxwell Building, The King's Buildings, Peter Guthrie Tait Road, Edinburgh, EH9 3FD, UK.

3 Deceased.

Corresponding author: Dr C. M. Pooley

Address: The Roslin Institute, The University of Edinburgh, Midlothian, EH25 9RG, UK

Email: christopher.pooley@roslin.ed.ac.uk

Tel: +44 (0)131 651 9100

ORCID: 0000-0002-8779-4477

Funding

This research was funded by the Scottish Government's Rural and Environment Science and Analytical Services Division (RESAS).

Abstract

Markov chain Monte Carlo (MCMC) is widely used for Bayesian inference in models of complex systems. Performance, however, is often unsatisfactory in models with many latent variables due to so-called poor mixing, necessitating development of application specific implementations. This limits rigorous use of real-world data to inform development and testing of models in applications ranging from statistical genetics to finance. This paper introduces “posterior-based proposals” (PBPs), a new type of MCMC update applicable to a huge class of statistical models (whose conditional dependence structures are represented by directed acyclic graphs). PBPs generates large joint updates in parameter and latent variable space, whilst retaining good acceptance rates (typically 33%). Evaluation against standard approaches (Gibbs or Metropolis-Hastings updates) shows performance improvements by a factor of 2 to over 100 for widely varying model types: an individual-based model for disease diagnostic test data, a financial stochastic volatility model and mixed and generalised linear mixed models used in statistical genetics. PBPs are competitive with similarly targeted state-of-the-art approaches such as Hamiltonian MCMC and particle MCMC, and importantly work under scenarios where these approaches do not. PBPs therefore represent an additional general purpose technique that can be usefully applied in a wide variety of contexts.

Keywords: Posterior-based proposal; Markov chain Monte Carlo; Bayesian inference; mixed model; stochastic volatility; statistical genetics;

1 Introduction

Markov chain Monte Carlo (MCMC) techniques allow correlated samples to be drawn from essentially any probability distribution by iteratively generating successive values of a carefully constructed Markov chain. This flexibility has led MCMC to become the method of choice for inferring model parameters under Bayesian inference [1]. However, for high dimensional systems (*e.g.* where inference is over many tens, hundreds or even thousands of variables), MCMC often suffers from a problem known as “poor mixing”. This manifests itself as a high degree of correlation between consecutive samples along the Markov chain, so requiring a very large number of iterations to adequately explore the posterior [2]. This limitation is of practical importance, because it restricts the possible models to which MCMC can realistically be applied. The focus of this paper is to introduce and explore a new approach that helps alleviate these mixing problems, thus reducing the computational time necessary to generate accurate inference. This approach has practical advantages over existing methodologies that aim to address the same problem [3-5].

In Bayesian inference the posterior distribution $\pi(\theta, \xi | y)$ represents the state of knowledge concerning the parameters θ and latent variables ξ of a given stochastic model taking into account data y . Using Bayes’ theorem this posterior distribution can be expressed as

$$\pi(\theta, \xi | y) = \frac{\pi(y | \xi, \theta) \pi(\xi | \theta) \pi(\theta)}{\pi(y)}, \quad (1)$$

where $\pi(y | \xi, \theta)$ is here referred to as the observation model, $\pi(\xi | \theta)$ is the latent process (*i.e.* the model that is usually the focus of interest) likelihood, $\pi(\theta)$ is the prior distribution (representing the state of knowledge prior to data y being considered), and $\pi(y)$ is a constant factor known as the model evidence [6].

An MCMC implementation of Bayesian inference aims to produce samples from the posterior, *i.e.* a list of parameter values θ^i and latent variables ξ^i distributed in accordance with Eq.(1). This is achieved by sequentially proposing some change to the current state θ^i and/or ξ^i to generate θ^p and ξ^p , and accepting or rejecting this change with a Metropolis-Hastings (MH) probability to create the next member on the list, *i.e.* θ^{i+1} and ξ^{i+1} [7]. Note, in some instances it is possible to probabilistically generate samples directly, *e.g.* via Gibbs sampling [8] or slice sampling [9], without the need for an accept/reject step¹. The term Monte Carlo refers to the probabilistic nature of these updates that form a Markov chain, *i.e.* step $i+1$ in the chain only depends on the state at the previous step.

¹ In these cases the MH acceptance probability is exactly one.

A typical approach is to sequentially update each parameter and latent variable separately. Figure 1(a) illustrates the problem of poor mixing resulting from implementing this “standard” MCMC when there is a strong dependency between latent variables and model parameters. The dark shaded area represents high posterior probability² as a function of θ and ξ . Consider first fixing θ and making changes to ξ , as shown by the dashed line in Fig. 1(a). Because MCMC samples are probabilistically constrained to lie in the shaded region, the chain will make limited progress even for a large number of MH updates. Similarly, changes to θ whilst fixing ξ will be restricted to move along horizontal lines, which are again limited in scope. A typical output from an MCMC algorithm which independently updates parameters and latent variable is illustrated in Fig. 1(b), which shows the trace plot for one of the variables in θ . Thousands of MH updates are potentially needed to generate just one uncorrelated effective sample from the posterior.

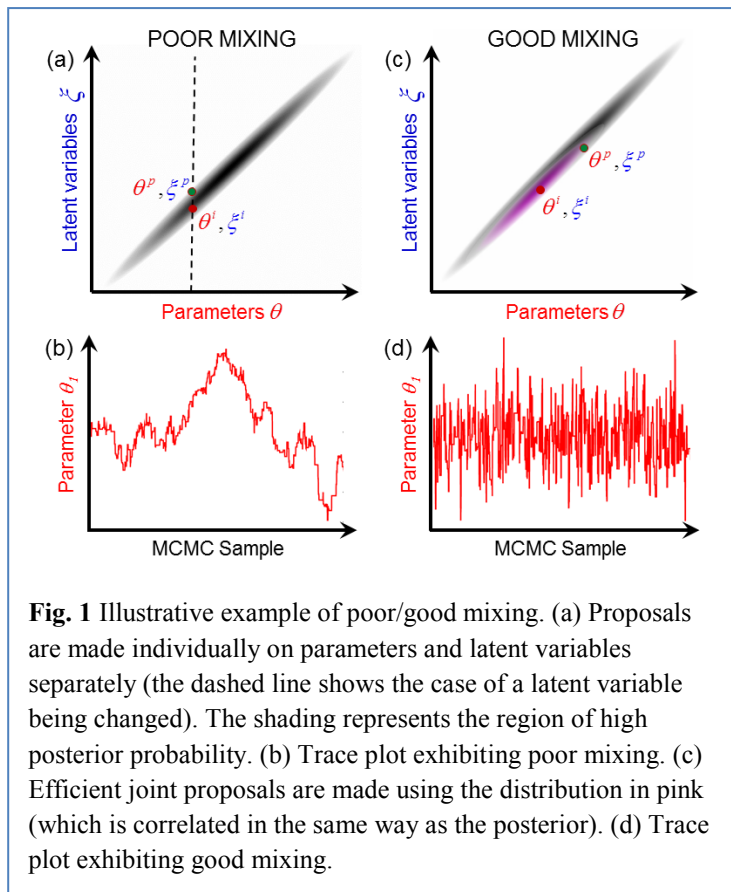


Fig. 1 Illustrative example of poor/good mixing. (a) Proposals are made individually on parameters and latent variables separately (the dashed line shows the case of a latent variable being changed). The shading represents the region of high posterior probability. (b) Trace plot exhibiting poor mixing. (c) Efficient joint proposals are made using the distribution in pink (which is correlated in the same way as the posterior). (d) Trace plot exhibiting good mixing.

The way out of this sorry state of affairs is shown in Fig. 1(c). Here the proposals are performed *jointly* in parameter and latent variable space (as indicated by the pink shaded region) and share a similar correlated structure to the posterior itself. In this case, proposals can jump much further without the posterior probability becoming negligibly small. Consequently, as illustrated in Fig. 1(d), successive samples are less correlated and fewer are needed to be representative of the posterior.

Various techniques to perform joint updates have been proposed in the literature. For example Particle MCMC (PMCMC) [3] samples a new set of parameters θ^p relative to θ^i and then sets about generating ξ^p . This is achieved by directly sampling from the model $\pi(\xi|\theta^p)$ multiple times, with each instance referred to as a “particle”. The final result is built up in a series of stages that sequentially take into account a larger fraction of the data y . At the end of each stage those particles which agree well with the sequentially introduced observations are duplicated at the expense of those which don’t agree so well (so-called particle filtering). Whilst this method exhibits very good mixing, computational speed is often compromised because the number of particles needed to generate a reasonable acceptance probability can be very large³ [10]. Furthermore, PMCMC is limited to scenarios in which data is sequentially ordered (such as in time series data).

² Note, this diagram is purely schematic, as θ and ξ are usually multi-dimensional quantities.

³ Potentially leading to detrimentally large computational memory requirements.

Approximate Bayesian Computation (ABC) [3] also samples directly from the model, but rather than fitting the data to the samples through a full observation model, as in Eq.(1), here the fit with the data is characterised by a much simpler distance measure χ . Often χ is specifically chosen such that a substantial proportion of simulated samples contribute to the final result. Such an approach, however, comes at a significant cost, because ABC generates only approximate, rather than exact, draws from the posterior [11]. Furthermore, doubts have been cast on ABC's ability to accurately perform model selection [11, 12].

In Hamiltonian MCMC (HMCMC) [4] θ^i and ξ^i are dynamically changed through a series of small intermediary steps (which take into account local gradients in the log of the posterior probability) to reach θ^p and ξ^p . This final state is then accepted or rejected with an overall MH probability. This, again, produces good mixing (due to the fact that θ^i, ξ^i and θ^p, ξ^p can be widely separated), but its efficiency is critically dependent on the number of intermediary steps needed for a sufficiently high acceptance rate [4]. Although recent improvements have helped to optimise this technique (most notably the "No-U-turn sampler" introduced in [13]), HMCMC is applicable to only those models for which θ and ξ are continuous quantities. Consequently, it is not well suited to tackle models with discrete variables, *e.g.* disease status [14], or variable dimension number, *e.g.* event data [15].

Another approach is to develop a non-centred parameterisation [5, 16, 17] in which a new set of latent variables ξ' (whose distributions are typically independent of the model parameters θ) are introduced. These new variables are related to the original latent variables through some deterministic function $\xi = h(\xi', \theta, y)$. MCMC implemented using this re-parameterisation can lead to improved mixing [17]. In this case, proposed changes to ξ' can be thought of as joint proposals in both ξ and θ .

This paper introduces a new class of MCMC proposal valid for the vast majority of statistical models (Section 2). We refer to these as "posterior-based proposals" (PBPs, Sections 3), as they are constructed with the aid of importance distributions (Section 4) which approximate the posterior. PBPs enable joint updates to both θ and ξ (unlike standard approaches), are fast (*i.e.* they don't require multiple particles like PMCMC), accurate (*i.e.* they draw samples from the true posterior, unlike ABC) and they can be applied to continuous or discrete state space models (unlike HMCMC). A further novelty in PBPs is that they not only account for correlations between θ and ξ inherent to the model, but can also take into account the data (unlike non-centred re-parameterisations). Application to models used in disciplines ranging from statistical genetics to epidemiology to finance demonstrate that PBPs potentially offer considerable improvements in performance over standard approaches (Section 5).

2 Broadly applicable model framework

PBPs are applicable to any statistical model whose conditional dependence structure can be represented by a Direct Acyclic Graph (DAG) [18], as illustrated in Fig. 2. This encompasses a vast range of statistical models including mixed models [19], generalised linear mixed models [20] and discrete time Markov processes [21]. A key property of DAGs is that the indexes for the latent variables e can be ordered such that each element ξ_e is conditionally dependant on only those other elements with lower index $\xi_{e' < e}$ (a property known as a topological ordering)⁴.

Simulation results from sequentially sampling each latent variable ξ_e (starting from $e=1$ up to $e=E$) from a set of model-defining univariate probability distributions $\pi(\xi_e | \xi_{e' < e}, \theta)$. Consequently, the latent process likelihood in Eq.(1) can be expressed as

$$\pi(\xi | \theta) = \prod_{e=1}^E \pi(\xi_e | \xi_{e' < e}, \theta). \quad (2)$$

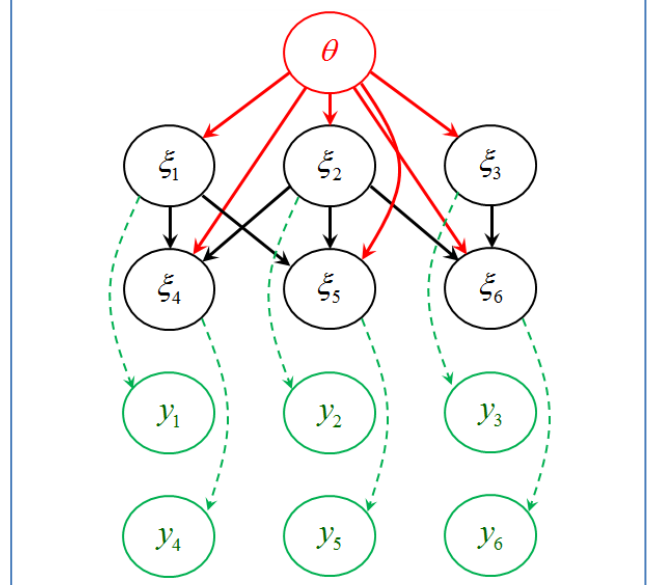


Fig. 2 A directed acyclic graph (DAG) illustrating a model with parameters θ , latent variables ξ and observations y . The arrows represent conditional dependencies. The model assumes that latent variables ξ_e (where e goes from 1 to $E=6$ in this example) are sampled from a set of univariate probability distributions $\pi(\xi_e | \xi_{e' < e}, \theta)$ and y_r are sampled from $\pi(y_r | \xi, \theta)$. Note, in general each observation y_r can depend on an arbitrary combination of ξ_e (this example shows the special case when y_r depends only on ξ_r).

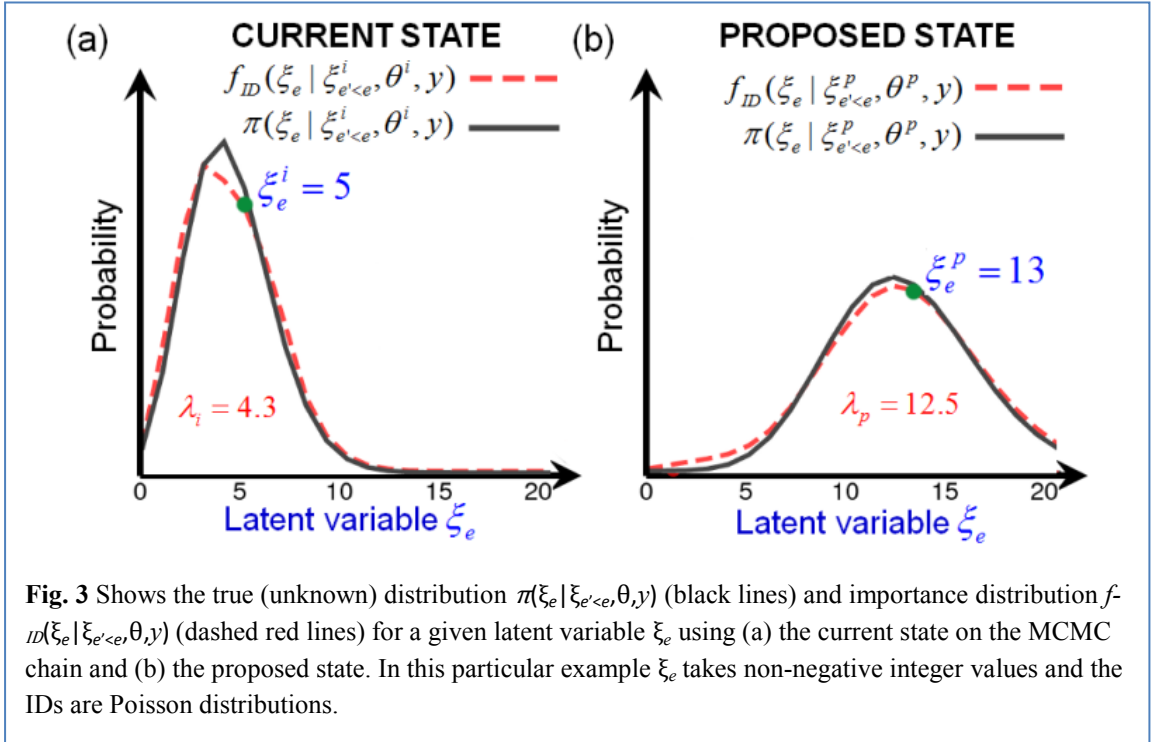


Fig. 3 Shows the true (unknown) distribution $\pi(\xi_e | \xi_{e' < e}, \theta, y)$ (black lines) and importance distribution $f_{ID}(\xi_e | \xi_{e' < e}, \theta, y)$ (dashed red lines) for a given latent variable ξ_e using (a) the current state on the MCMC chain and (b) the proposed state. In this particular example ξ_e takes non-negative integer values and the IDs are Poisson distributions.

⁴ The notation $\xi_{e' < e}$ denotes all elements in ξ with index smaller than e .

ID	Prob. Dist.	Posterior-based proposal
Poisson $\xi_e \sim Pois(\lambda)$	$\frac{\lambda^{\xi_e} e^{-\lambda}}{\xi_e!}$	$\lambda_p > \lambda_i$ $\xi_e^p = \xi_e^i + X$ where $X \sim Pois(\lambda_p - \lambda_i)$
		$\lambda_p \leq \lambda_i$ $\xi_e^p \sim B(\xi_e^i, \frac{\lambda_p}{\lambda_i})$
Normal $\xi_e \sim N(\mu, \sigma^2)$	$\frac{1}{\sqrt{2\pi\sigma^2}} e^{-\frac{(\xi_e - \mu)^2}{2\sigma^2}}$	$\sigma_p > \sigma_i$ $\xi_e^p \sim N(\mu_p + \alpha(\xi_e^i - \mu_i), \kappa(\sigma_p^2 - \sigma_i^2))$ where $\alpha^2 = \kappa + (1 - \kappa)\frac{\sigma_p^2}{\sigma_i^2}$
		$\sigma_p \leq \sigma_i$ $\xi_e^p \sim N(\mu_p + \alpha\frac{\sigma_p^2}{\sigma_i^2}(\xi_e^i - \mu_i), \kappa\frac{\sigma_p^2}{\sigma_i^2}(\sigma_i^2 - \sigma_p^2))$ where $\alpha^2 = \kappa + (1 - \kappa)\frac{\sigma_p^2}{\sigma_i^2}$ κ is a tuneable constant (typically set to 0.03, as discussed in Appendix F).
Exponential $\xi_e \sim Exp(r)$	$re^{-r\xi_e}$	$r_p > r_i$ $X \sim Exp(r_p - r_i)$, if $X > \xi_e^i$ then $\xi_e^p = X$ else $\xi_e^p = \xi_e^i$
		$r_p \leq r_i$ u is a random number between 0 and 1 if $u < 1 - \frac{r_p}{r_i}$ then $\xi_e^p = \xi_e^i + X$, $X \sim Exp(r_p)$ else $\xi_e^p = \xi_e^i$
Gamma $\xi_e \sim \Gamma(\alpha, \beta)$	$\frac{\beta^\alpha \xi_e^{\alpha-1} e^{-\beta\xi_e}}{\Gamma(\alpha)}$	$\alpha_p > \alpha_i$ $\xi_e^p = \frac{\beta_i}{\beta_p}(\xi_e^i + X)$ where $X \sim \Gamma(\alpha_p - \alpha_i, \beta_i)$
		$\alpha_p \leq \alpha_i$ $\xi_e^p = \frac{\beta_i}{\beta_p}\xi_e^i Y$ where $Y \sim Beta(\alpha_p, \alpha_i - \alpha_p)$
Beta $\xi_e \sim Beta(\alpha, \beta)$	$\frac{\Gamma(\alpha+\beta)}{\Gamma(\alpha)\Gamma(\beta)} \xi_e^{\alpha-1} (1-\xi_e)^{\beta-1}$	$\alpha_p > \alpha_i$ $\xi_e^p = 1 - (1 - \xi_e^i)X$ where $X \sim Beta(\beta_i + \alpha_i, \alpha_p - \alpha_i)$
		$\alpha_p \leq \alpha_i$ $\xi_e^p = \frac{\xi_e^i X}{1 - \xi_e^i(1 - X)}$ where $X \sim Beta(\alpha_p, \alpha_i - \alpha_p)$
		$\beta_p > \beta_i$ $\xi_e^p = \xi_e^i X$ where $X \sim Beta(\alpha_i + \beta_i, \beta_p - \beta_i)$
		$\alpha_p = \alpha_i$ $\xi_e^p = \xi_e^i X$ where $X \sim Beta(\beta_p, \beta_i - \beta_p)$
		$\beta_p \leq \beta_i$ $\xi_e^p = \frac{\xi_e^i}{\xi_e^i + (1 - \xi_e^i)X}$ where $X \sim Beta(\beta_p, \beta_i - \beta_p)$
		$\alpha_p = \alpha_i$ $\xi_e^p = \frac{\xi_e^i}{\xi_e^i + (1 - \xi_e^i)X}$ where $X \sim Beta(\beta_p, \beta_i - \beta_p)$
Bernoulli $\xi_e \sim Bern(z)$	$\Pr(\xi_e = 1) = z$ $\Pr(\xi_e = 0) = 1 - z$	$z_p > z_i$ if $\xi_e^i = 1$ set $\xi_e^p = 1$ else { if $u < \frac{z_p - z_i}{1 - z_i}$ then set $\xi_e^p = 1$ else $\xi_e^p = 0$ } where u is a random number between 0 and 1
		$z_p \leq z_i$ if $\xi_e^i = 0$ set $\xi_e^p = 0$ else { if $u < 1 - \frac{z_p}{z_i}$ then set $\xi_e^p = 0$ else $\xi_e^p = 1$ } where u is a random number between 0 and 1

Table 1(a): Shows how to sample the proposed latent variable ξ_e^p from ξ_e^i given some importance distribution (ID) functional form (left hand column), whose characteristic parameters change from some initial set to a proposed set.

ID	Prob. Dist.	Posterior-based proposal	
Binomial $\xi_e \sim B(N, z)$	$C_{\xi_e}^N z^{\xi_e} (1-z)^{N-\xi_e}$ where $C_n^N = \frac{N!}{n!(N-n)!}$	$z_p > z_i$	$\xi_e^p = \xi_e^i + X$ where $X \sim B(N_i - \xi_e^i, \frac{z_p - z_i}{1 - z_i})$
		$N_p = N_i$	
		$z_p \leq z_i$	$\xi_e^p \sim B(\xi_e^i, \frac{z_p}{z_i})$
		$N_p = N_i$	
		$N_p > N_i$	$\xi_e^p = \xi_e^i + X$ where $X \sim B(N_p - N_i, z_i)$
		$z_p = z_i$	
		$N_p \leq N_i$	$\xi_e^p \sim HG(N_i, N_p, \xi_e^i)$
		$z_p = z_i$	
Uniform $\xi_e \sim Uni(a, b)$	$\left. \begin{array}{l} \frac{1}{b-a} \\ 0 \end{array} \right\} \begin{array}{l} a \leq \xi_e \leq b \\ \xi_e < a \text{ or } \xi_e > b \end{array}$		$\xi_e^p = a_p + \left(\frac{\xi_e^i - a_i}{b_i - a_i} \right) (b_p - a_p)$
Geometric $\xi_e \sim Geom(z)$	$(1-z)^{\xi_e} z$	$z_p > z_i$	$X \sim Geom(\frac{z_p - z_i}{1 - z_i})$, if $X < \xi_e^i$ then $\xi_e^p = X$ else $\xi_e^p = \xi_e^i$
		$z_p \leq z_i$	u is a random number between 0 and 1 if $u < 1 - \frac{z_p}{z_i}$ then $\xi_e^p = \xi_e^i + 1 + X$, $X \sim Geom(z_p)$ else $\xi_e^p = \xi_e^i$
Negative Binomial $\xi_e \sim NB(r, z)$	$C_{\xi_e}^{\xi_e+r-1} z^{\xi_e} (1-z)^r$ where $C_n^N = \frac{N!}{n!(N-n)!}$	$z_p > z_i$	$\xi_e^p = \xi_e^i + q + X$ where $q \sim B(r_i, \frac{z_p - z_i}{1 - z_i})$, $X \sim NB(q, z_p)$
		$r_p = r_i$	
		$z_p \leq z_i$	$\xi_e^p \sim X$ where X is drawn from p.m.f.
		$r_p = r_i$	$\sum_{q=1}^r \left(C_q^r C_{\xi_e^i - X - q}^{\xi_e^i - X - 1} C_X^{X+r-1} / C_{\xi_e^i}^{\xi_e^i+r-1} \right) \left(1 - \frac{z_p}{z_i} \right)^q \left(\frac{z_p}{z_i} \right)^X$
		$r_p > r_i$	$\xi_e^p = \xi_e^i + X$ where $X \sim NB(r_p - r_i, z_i)$
		$z_p = z_i$	
		$r_p \leq r_i$	$\xi_e^p \sim NHG(\xi_e^i + r_i - 1, \xi_e^i, r_p)$
		$z_p = z_i$	
Lognormal $\xi_e \sim lnorm(\mu, \sigma^2)$	$\frac{1}{\xi_e \sqrt{2\pi\sigma^2}} e^{-\frac{(\log \xi_e - \mu)^2}{2\sigma^2}}$	$\sigma_p > \sigma_i$	$\log \xi_e^p \sim N\left(\mu_p + \alpha(\log \xi_e^i - \mu_i), \kappa(\sigma_p^2 - \sigma_i^2)\right)$ where $\alpha^2 = \kappa + (1 - \kappa) \frac{\sigma_p^2}{\sigma_i^2}$
		$\sigma_p \leq \sigma_i$	$\log \xi_e^p \sim N\left(\mu_p + \alpha \frac{\sigma_p^2}{\sigma_i^2} (\log \xi_e^i - \mu_i), \kappa \frac{\sigma_p^2}{\sigma_i^2} (\sigma_i^2 - \sigma_p^2)\right)$ where $\alpha^2 = \kappa + (1 - \kappa) \frac{\sigma_i^2}{\sigma_p^2}$
Logistic $\xi_e \sim logistic(\mu, s)$	$\frac{e^{-\frac{\xi_e - \mu}{s}}}{s(1 + e^{-\frac{\xi_e - \mu}{s}})}$		$\xi_e^p = \mu_p + \left(\xi_e^i - \mu_p \right) \frac{S_p}{S_i}$

Table 1(b): Here draws from the hypergeometric distribution $X \sim HG(N, K, n)$ have p.m.f.

$C_X^K C_{n-X}^{N-K} / C_n^N$ and from the negative hypergeometric distribution $X \sim NHG(N, K, r)$ have p.m.f.

$C_X^{X+r-1} C_{K-X}^{N-r-X} / C_K^N$.

3 Posterior-based proposals (PBPs)

3.1 Aim

PBPs first propose a new set of parameters θ^p relative to θ^i and then generate ξ^p by means of stochastically *modifying* ξ^i to account for this change in parameters (note, this is in stark contrast to PMCMC which aims to *sample* ξ^p directly from $\pi(\xi | \theta^p, y)$ without reference to ξ^i or θ^i). The novel PBP process involves sequentially sampling each latent variable ξ_e^p from $e=1$ up to E , and makes use of so-called ‘‘importance distributions’’ (IDs) applied to both the initial and proposed states. These importance distributions $f_{ID}(\xi_e | \xi_{e' < e}, \theta, y)$ are approximations to the posterior distributions $\pi(\xi_e | \xi_{e' < e}, \theta, y)$ used in importance sampling (see Appendix A for further details). For clarity we leave a discussion of how these approximations are made in practice until Section 4.

3.2 Example

We first run through an illustrative example of a PBP and then provide a general description in Section 3.3. Figure 3 shows hypothetical distributions for a particular value of e for which ξ_e takes non-negative integer values. Here the black lines represent the true (unknown) distributions for the current $\pi(\xi_e | \xi_{e' < e}, \theta^i, y)$ and proposed $\pi(\xi_e | \xi_{e' < e}, \theta^p, y)$ states, respectively. Since these curves are approximately Poisson distributed⁵, the IDs are taken to be Poisson (as shown by the red dashed lines in Fig. 3) with probability mass functions

$$\begin{aligned} f_{ID}(\xi_e | \xi_{e' < e}, \theta^i, y) &= \frac{e^{-\lambda_i} \lambda_i^{\xi_e}}{\xi_e!}, \\ f_{ID}(\xi_e | \xi_{e' < e}, \theta^p, y) &= \frac{e^{-\lambda_p} \lambda_p^{\xi_e}}{\xi_e!}. \end{aligned} \quad (3)$$

These are characterised by ‘‘expected event number’’ parameters λ_i and λ_p , which themselves are functionally dependent on $(\xi_{e' < e}^i, \theta^i, y)$ and $(\xi_{e' < e}^p, \theta^p, y)$, respectively (see Section 4).

A unique feature of PBPs is that the sampling distribution for ξ_e^p crucially depends on the relative size of λ_p and λ_i . When $\lambda_p > \lambda_i$ (as it is in Fig. 3) ξ_e^p is generated by adding a Poisson distributed variable onto ξ_e^i with expected event number given by the *difference* between λ_p and λ_i :

$$\xi_e^p = \xi_e^i + X \quad \text{where} \quad X \sim \text{Pois}(\lambda_p - \lambda_i) \quad (4)$$

(e.g. in Fig. 3 a random Poisson sample $X=8$ results in $\xi_e^p = \xi_e^i + X = 13$). Such an approach makes sense, because adding an approximately Poisson distributed quantity with expected event number λ_i , to one with expected event number $\lambda_p - \lambda_i$, gives an approximately Poisson distributed variable with expected event number λ_p , as required by ξ_e^p on the left hand side of Eq.(4). Thus, Eq.(4) modifies ξ_e^i to generate ξ_e^p accounting for the change in λ .

On the other hand, when $\lambda_p \leq \lambda_i$ the actual number of events in the proposed state ξ_e^p should be less than in the initial state ξ_e^i , because the expected number of events parameter λ has reduced.

⁵ A Poisson distribution expresses the probability a given number of events occur in a fixed interval of time, assuming that events occur at a constant rate.

Specifically each existing event in ξ_e^i is retained in ξ_e^p with probability λ_p/λ_i , which is equivalent to sampling ξ_e^p from the following binomial distribution⁶

$$\xi_e^p \sim B(\xi_e^i, \frac{\lambda_p}{\lambda_i}). \quad (5)$$

Together, the two potential sampling schemes for ξ_e^p in Eqs.(4) and (5) (selected depending on whether λ_p is bigger or smaller than λ_i) make up the PBP proposal in cases in which the ID is Poisson. This is summarised by the first line in Table 1.

3.3 General approach

In general the choice of ID will depend on the distribution $\pi(\xi|\theta^p, y)$, which itself is model dependent. If, for example, $\pi(\xi_e|\xi_{e'<e}, \theta^i, y)$ is better represented by a normal ID, the PBP sampling procedure is taken from the second line in Table 1. In all, Table 1 summarises sampling schemes for twelve different ID functional forms, each corresponding to probability distributions commonly used in statistical models. These schemes are specifically designed to satisfy the following two conditions:

$$\text{Condition 1: } \frac{f_{ID}(\xi_e^p | \xi_{e'<e}^p, \theta^p, y)}{f_{ID}(\xi_e^i | \xi_{e'<e}^i, \theta^i, y)} \frac{g(\xi_e^i)}{g(\xi_e^p)} = 1, \quad (6)$$

$$\text{Condition 2: } \xi_e^p \rightarrow \xi_e^i \text{ as } \theta^p \rightarrow \theta^i,$$

where $g(\xi_e^p)$ is the probability of sampling latent variables ξ_e^p starting from state i , and $g(\xi_e^i)$ is the probability of sampling ξ_e^i when proposing state i from p . Condition 1 ensures that if ξ_e^i is a random sample from $f_{ID}(\xi_e | \xi_{e'<e}^i, \theta^i, y)$ then ξ_e^p will, by construction, be a random sample from $f_{ID}(\xi_e | \xi_{e'<e}^p, \theta^p, y)$ (albeit by design correlated with ξ_e^i). Condition 2 guarantees that proposals with small jumps in parameter space have an acceptance probability close to one.

Note, condition 1 can trivially be solved by sampling directly from the IDs

$$\begin{aligned} g(\xi_e^p) &= f_{ID}(\xi_e^p | \xi_{e'<e}^p, \theta^p, y), \\ g(\xi_e^i) &= f_{ID}(\xi_e^i | \xi_{e'<e}^i, \theta^i, y), \end{aligned} \quad (7)$$

but this doesn't satisfy condition 2 and turns out to usually be inefficient⁷. Deriving sampling schemes which also satisfy condition 2 is a non-trivial task guided by intuition and trial and error. The validity of Eqs.(6) for both Poisson and normal IDs is explicitly demonstrated in Appendix B.

⁶ If N represents the total number of experiments and p is the success probability of each experiment then $B(N, p)$ samples the number of successes.

⁷ This approach is akin to standard importance sampling and typically leads to very low acceptance rates for high dimensional models.

3.4 Algorithm

We now describe the general algorithm used to implement PBPs:

POSTERIOR-BASED PROPOSALS

Step 1: Generate θ^p – A proposed set of parameter values is drawn from a multivariate normal (MVN) distribution centred on the current set of parameters in the chain θ^i

$$\theta^p \sim N(\theta^i, j^2 \Sigma^\theta), \quad (8)$$

where Σ^θ is a numerical approximation to the covariance matrix for $\pi(\theta|y)$ and j is a tuneable jumping parameter (estimation of Σ^θ and optimisation of j are achieved during an initial “adaptation” period, as explained in Appendix C). (Note, performing a joint update on all parameters instead of each individually helps to alleviate poor mixing due to strong parameter correlations in $\pi(\theta|y)$).

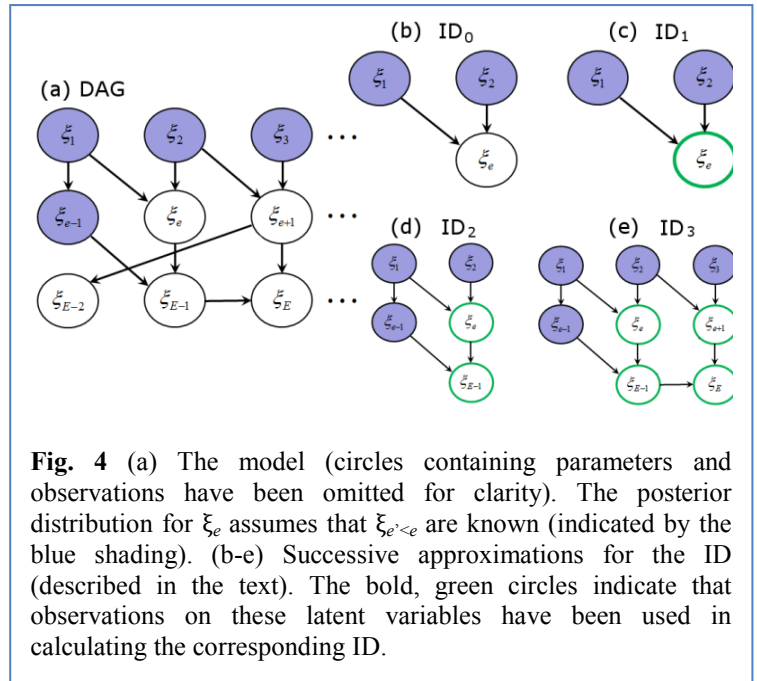
Step 2: Generate ξ^p – We take each latent variable ξ_e in turn (starting from $e=1$ up to $e=E$) and calculate the characteristic quantities defining the IDs for the initial and proposed states (e.g. in the Poisson case this would be λ_i and λ_p), as described in Section 4. ξ_e^p is then sampled using specially design proposals outlined in Table 1 (note, this table contains separate lines referring to different potential ID functional forms). This sampling procedure is at the heart of PBPs and represents the key novelty of this approach.

Step 3: Accept or reject joint proposal for θ^p and ξ^p – With MH probability (see Appendix D)

$$P_{MH} = \min \left\{ 1, \frac{\pi(y|\xi^p, \theta^p) \pi(\xi^p|\theta^p) \pi(\theta^p)}{\pi(y|\xi^i, \theta^i) \pi(\xi^i|\theta^i) \pi(\theta^i)} \prod_{e=1}^E \frac{f_{ID}(\xi_e^i|\xi_{e'<e}^i, \theta^i, y)}{f_{ID}(\xi_e^p|\xi_{e'<e}^p, \theta^p, y)} \right\}. \quad (9)$$

Further insights into the PBP procedure are given in Appendix E.

PBPs, by design, result in ξ^p exhibiting correlation with ξ^i (indeed, if $\theta^p = \theta^i$ then ξ^p is exactly the same as ξ^i , as required by Eq.(6)). The PBP MCMC algorithm used in this paper mitigates against these correlations by performing PBPs interspersed with standard updates for the latent variables⁸ every U steps. Appendix H shows that mixing is not sensitive to the exact value for U , and is approximately optimised when $U=4$ (as subsequently used).



⁸ Which passes through each latent variable and performs a Gibbs or random walk MH update.

4 Generating importance distributions (ID)

For each latent variable ξ_e , the distribution we wish to approximate is $\pi(\xi_e | \xi_{e' < e}, \theta, y)$, *i.e.* the posterior probability distribution for ξ_e given $\xi_{e' < e}$, parameters θ , and data y . This distribution can be expressed as

$$\pi(\xi_e | \xi_{e' < e}, \theta, y) = \int \int \pi(\xi_{d \geq e} | \xi_{e' < e}, \theta, y) d\xi_E \dots d\xi_{e+1}, \quad (10)$$

where $\pi(\xi_{d \geq e} | \xi_{e' < e}, \theta, y)$ is the joint posterior distribution for latent variables with index e and above (conditional on everything else). The integrals in Eq.(10) successively marginalise over the unknown latent variables, starting with the last ξ_E all the way back to ξ_{e+1} . Using Bayes' theorem and Eq.(1), the integrand in Eq.(10) can be expressed as

$$\begin{aligned} \pi(\xi_{d \geq e} | \xi_{e' < e}, \theta, y) &\propto \pi(y | \xi, \theta) \pi(\xi_{d \geq e} | \xi_{e' < e}, \theta) \\ &\propto \pi(\xi_e | \xi_{e' < e}, \theta) \pi(y | \xi, \theta) \prod_{d=e+1}^E \pi(\xi_d | \xi_{e' < d}, \theta). \end{aligned} \quad (11)$$

For now making the simplification that one observation is made per latent variable, *i.e.*

$$\pi(y | \xi, \theta) = \prod_{e=1}^E \pi(y_e | \xi_e, \theta), \quad (12)$$

and substituting Eq.(11) into Eq.(10) gives

$$\begin{aligned} \pi(\xi_e | \xi_{e' < e}, \theta, y) &\propto \pi(\xi_e | \xi_{e' < e}, \theta) \pi(y_e | \xi_e, \theta) \\ &\times \int \int \prod_{d=e+1}^E \pi(\xi_d | \xi_{e' < d}, \theta) \pi(y_d | \xi_d, \theta) d\xi_E \dots d\xi_{e+1}. \end{aligned} \quad (13)$$

Analytically performing these integrals is usually not possible. However different levels of approximation can be made depending on the point at which the expression on the right hand side of Eq.(13) is truncated. This leads to a family of importance distributions with increasing accuracy (as illustrated in Fig. 4):

ID₀

By taking just the first term on the right hand side of Eq.(13), the ID is simply set to the distribution from the model itself⁹

$$f_{ID_0}(\xi_e | \xi_{e' < e}, \theta) = \pi(\xi_e | \xi_{e' < e}, \theta). \quad (14)$$

Note, this can only be done provided the model distribution $\pi(\xi_e | \xi_{e' < e}, \theta)$ has a functional form belonging to one of the possibilities in Table 1 (or alternatively a new PBP sampling scheme based on the model distribution is created which satisfies the conditions in Eq.(6)). If this cannot be achieved, the functional form for ID₀ is chosen to match $\pi(\xi_e | \xi_{e' < e}, \theta)$ as closely as possible.

The calculation of ID₀, as illustrated in Fig. 4(b), involves only those latent variables on which ξ_e is conditionally dependant. PBPs using ID₀ are equivalent to model-based proposals[10] (MBPs), and their MH acceptance probability from Eq.(9) simplifies to

⁹ Note, the proportionality sign in Eq.(13) becomes an equality sign because $\pi(\xi_e | \xi_{e' < e}, \theta)$ is normalised.

$$P_{MH} = \min \left\{ 1, \frac{\pi(y|\xi^p, \theta^p)\pi(\theta^p)}{\pi(y|\xi^i, \theta^i)\pi(\theta^i)} \right\}. \quad (15)$$

ID₁

The ID accuracy is improved by using the first two terms on the right hand side of Eq.(13)

$$f_{ID_1}(\xi_e | \xi_{e' < e}, \theta, y) = c\pi(\xi_e | \xi_{e' < e}, \theta)\pi(y_e | \xi_e, \theta), \quad (16)$$

where c is a normalising factor. Calculation of ID₁, as illustrated in Fig. 4(c), includes not only those latent variables on which ξ_e is dependant, but also the observation y_e on ξ_e itself (as indicated by the green circle)¹⁰.

ID₂

Including observations on those latent variables which depend on ξ_e , e.g. ξ_{E-1} in Fig. 4(d), Eq.(13) now gives the improved approximation

$$f_{ID_2}(\xi_e | \xi_{e' < e}, \theta, y) = c\pi(\xi_e | \xi_{e' < e}, \theta)\pi(y_e | \xi_e, \theta) \int \pi(\xi_{E-1} | \xi_{e' < E-1}, \theta)\pi(y_{E-1} | \xi_{E-1}, \theta) d\xi_{E-1}. \quad (17)$$

Higher order approximations (*i.e.* ID_{n>2} which take into account successively more of the model and data¹¹) usually prove to be too computationally expensive to be efficient.

Choosing ID

Choosing which level of ID to optimise PBPs involves a trade-off between the computational cost of generating IDs with the size of posterior jumps (and hence improvement in mixing) they allow. Unfortunately determining *a priori* which option is best is challenging. Indeed, in the results section below we find examples for which ID₁ and ID₂ each represent optimum solutions for different problems.

The classification scheme presented above is based on models which have one observation per latent variable. For models in which this is not the case, generation of IDs relies on approximating the following expression:

$$\pi(\xi_e | \xi_{e' < e}, \theta, y) \propto \pi(\xi_e | \xi_{e' < e}, \theta) \int \int \pi(y | \xi, \theta) \prod_{d=e+1}^E \pi(\xi_d | \xi_{e' < d}, \theta) d\xi_E \dots d\xi_{e+1}. \quad (18)$$

This may or may not be computationally challenging, depending on the scenario considered. However, provided the model itself makes use of the distributions in Table 1, using ID₀ (*i.e.* MBPs) is always possible.

5 Empirical evaluation

We now investigate the relative computational performance of PBPs compared to standard MCMC approaches applied to four contrasting model types. In each case we examine algorithm performance for parameter inference from data simulated from the models in question. Results

¹⁰ This relies on the product of model and observation probability distributions being contained within Table 1. If this is not the case then some level of approximation is necessary.

¹¹ ID_n is the approximation to Eq.(13) in which those latent variables ξ_d that are $n-1$ or fewer arrows away from ξ_e (along with any latent variables on which they depend) are included in the integral.

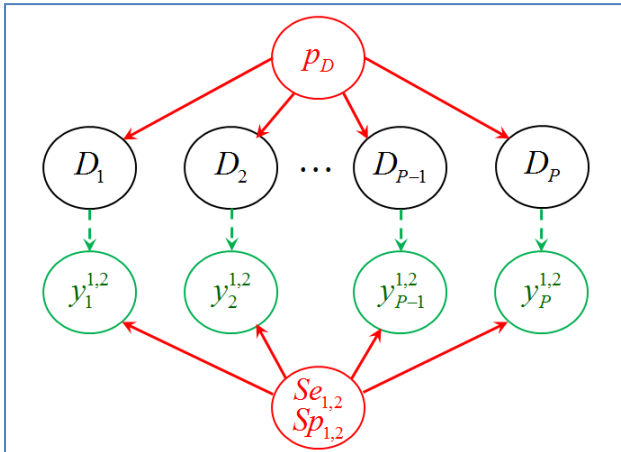


Fig 5. The disease diagnostic test model (Section 5.1) with probability of disease p_D , true disease status D_e (1/0 denoting infected/uninfected), and observed disease status as measured from two diagnostic tests $y_{e,1,2}$ (which have sensitivities $Se_{1,2}$ and specificities $Sp_{1,2}$).

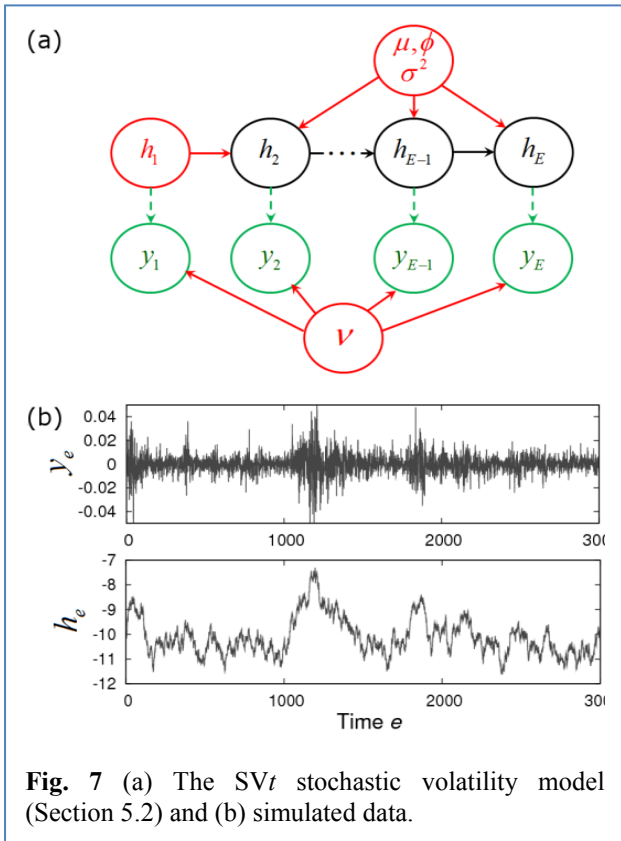


Fig. 7 (a) The SVt stochastic volatility model (Section 5.2) and (b) simulated data.

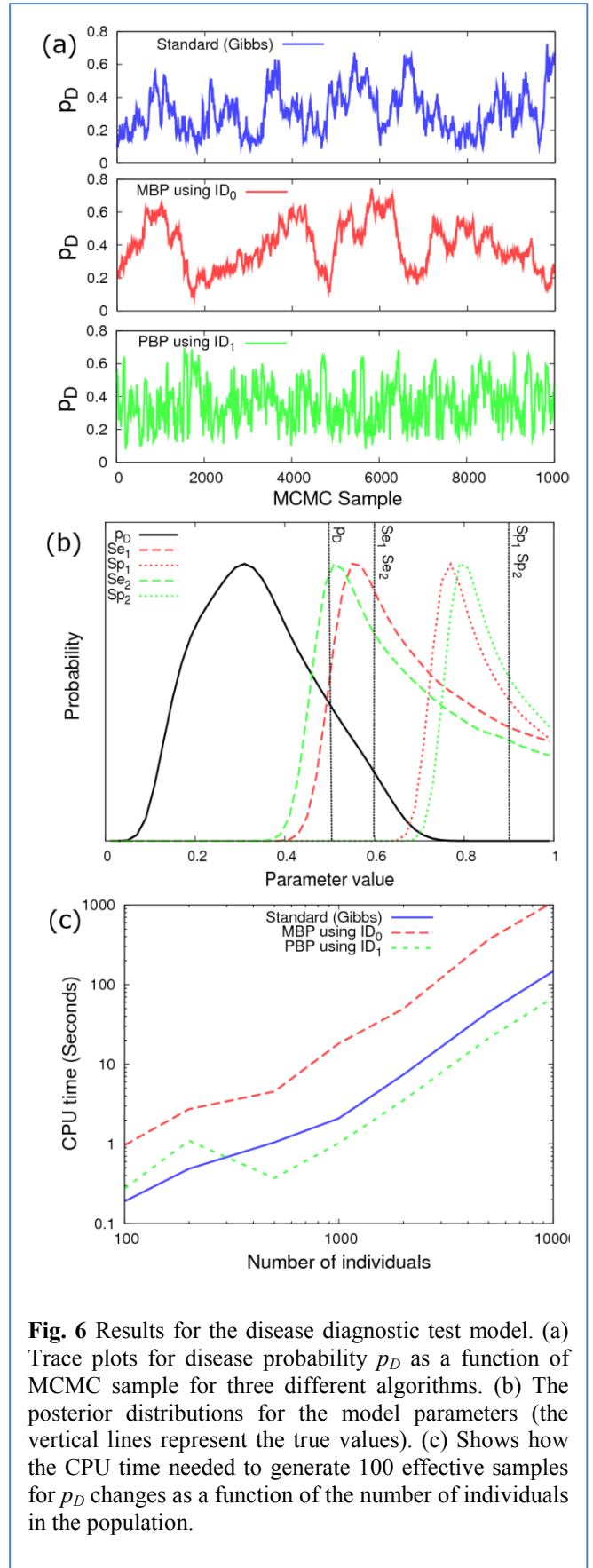


Fig. 6 Results for the disease diagnostic test model. (a) Trace plots for disease probability p_D as a function of MCMC sample for three different algorithms. (b) The posterior distributions for the model parameters (the vertical lines represent the true values). (c) Shows how the CPU time needed to generate 100 effective samples for p_D changes as a function of the number of individuals in the population.

shown are based on 10^6 MCMC sample “updates” (where each update makes changes to all the latent variables and model parameters) preceded by 10^4 discarded samples from a burn-in/adaptation period (see Appendix C). One way to measure MCMC efficiency is to calculate the “effective sample size” [2] (see Appendix I), and here we calculate the computational time for any given algorithm to generate 100 effective posterior samples¹² of a given parameter. Unless otherwise stated, uninformative flat priors are assumed.

5.1 Inferring disease prevalence and diagnostic test performance

Suppose we aim to estimate the disease prevalence (fraction of infected) p_D in a population of P individuals using cross-sectional diagnostic test results. Such diagnostic tests are typically imperfect, and characterised by a sensitivity Se (the probability of a positive test result given an infected individual) and specificity Sp (the probability of a negative test result given uninfected). Suppose Se and Sp are unknown. In the absence of a gold standard defining which individuals are truly infected, inference is only possible when two or more independent tests are recorded per individual (due to confounding). Here we assume that results are available from two tests, labelled $t=\{1,2\}$. The model is shown in Fig. 5 and described in detail along with development of PBP proposals in Appendix J. We note that this model could be embedded in more complex models, *e.g.* fitted to data from capture-mark-recapture programmes [22].

Speed comparison

Simulated data was created using $p_D=0.5$, $Se_1=Se_2=0.6$ and $Sp_1=Sp_2=0.9$ for $P=1000$ individuals. Inference was then performed using MBP/PBP MCMC approaches as well as standard Gibbs sampling. Figure 6(a) shows how posterior samples for p_D vary as each of the three algorithms progress. By binning these samples, the marginal posterior distributions for p_D can be generated, as shown in Fig. 6(b) (which also shows results for the other model parameters). These distributions contain the known values used to generate the data (denoted by vertical black lines), indicating successful inference.

It is important to note that in the limit of infinite MCMC sample number each of the three algorithms is expected to generate exactly the same set of marginal distributions (*i.e.* those shown in Fig. 6(b)). However the speed with which they converge *does* vary. For example, Fig. 6(c) shows how the computational time (*i.e.* the CPU time to generate 100 effective samples) to infer p_D increases with population size. Here we find that MBPs (ID₀) actually performs worse than the standard Gibbs approach, however when observations are incorporated (ID₁) the resultant PBP algorithm is around two times faster than Gibbs sampling (at least when the number of individuals is large). Although mixing is greatly improved, as is evident from Fig. 6(a), this is offset by the computational overhead associated with each PBP. This simple example demonstrates a possible modest improvement in computational speed when using PBPs compared to a standard Gibbs approach. The next example, however, shows that much larger potential gains can be made.

5.2 Fitting dynamic models: a stochastic volatility model

Stochastic volatility (SV) models are used to capture time-varying volatility on financial markets, and are essential tools in risk management, asset pricing and asset allocation [23]. In economics, a “logarithmic rate of return” can be defined by $y_e=\log(V_{e+1}/V_e)$, where V_e is the price of an asset (*e.g.* a

¹² Simulation and inference were averaged over ten separate runs to help remove data-dependent noise.

share) on day e . Consequently, when y_e is positive it means that on day $e+1$ the asset goes up in price, but when it is negative it goes down. One way to capture time variation in y_e is through the so-called SVt model [24]

$$\begin{aligned} y_e &= e^{h_e/2} u_e, \\ h_e &= \mu + \phi(h_{e-1} - \mu) + \eta_e, \end{aligned} \quad (19)$$

where u_e are i.i.d. with a Student's t -distribution (characterised by parameter ν) and η_e are i.i.d. normal (with zero mean and variance σ^2). Note, if h_e is fixed (*i.e.* $\sigma=0$), the logarithmic rate of return y_e would simply be sampled asymptotically from a distribution with fixed variance, or "volatility". The introduction of time variation in the variable h_e , whose temporal correlations are measured by $0 < \phi < 1$, means that y_e experiences stochastic volatility, *i.e.* periods when there are large variations in asset price, and other periods when there isn't much variation.

The SVt model is represented in Fig. 7(a). Simulated data was created using $\mu=-10$, $\phi=0.99$, $\nu=12$, $\sigma^2=0.0121$ (which are parameter values based on estimates made from the S&P 500 index [23]). Figure 7(b) shows the time variation in y_e and h_e (observe how changes in h_e correspond to changes in the volatility of y_e) over $E=3000$ days. A detailed development of PBP proposals for this model is given in Appendix K.

Speed comparison

Bayesian inference from the simulated data in Fig. 7(b) identifies marginal posterior distributions which contain the true parameter values, as indicated by black vertical lines in Fig 8(a). For each algorithm Fig. 8(b) shows how the computational time to infer σ^2 varies with the correlation parameter ϕ used to generate the data (with all other parameters fixed as above). The standard algorithm is at its fastest when $\phi \sim 1$ but slows down considerably as $\phi \rightarrow 0$, whereas the opposite holds for the MBP/PBP algorithms¹³. In addition, ID₁ is found to be faster than ID₂ or ID₀. For real financial markets ϕ is within the range 0.95 to 0.99 [23], reflecting a high degree of persistence in

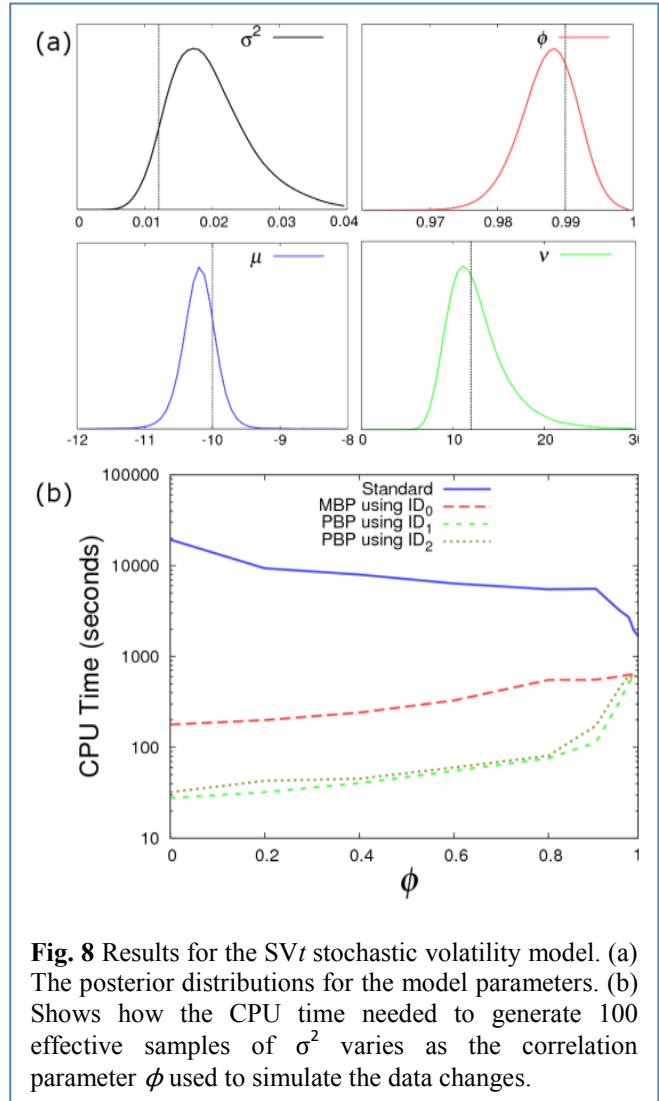


Fig. 8 Results for the SVt stochastic volatility model. (a) The posterior distributions for the model parameters. (b) Shows how the CPU time needed to generate 100 effective samples of σ^2 varies as the correlation parameter ϕ used to simulate the data changes.

¹³ The reason PBPs become slower as $\phi \rightarrow 1$ is that (due to correlations introduced by ϕ) $\pi(\xi_e | \xi_{e' < e}, \theta, y)$ is expected to depend on observations up to around $1/(1-\phi)$ days ahead. In contrast, ID_n only includes observations up to $n-1$ days ahead, which is typically a much shorter interval.

volatility. This corresponds to PBP running between four and ten times faster than the standard approach. However, the left hand side of Fig. 8(b) clearly demonstrates the existence of regimes for which PBPs are faster by a factor exceeding 100.

5.3 Mixed models (MMs)

MMs [25] explain observations in terms of both “fixed effects” (*e.g.* individual attributes such as gender or disease status) and “random effects” (which account for random uncontrollable factors within a study, *e.g.* variation in student grades as a result of variation in the quality of schools). MMs are useful in a wide variety of applications in the physical, biological and social sciences [26-29]. They assume that a vector of N measurements y can be decomposed into three contributions:

$$y = X\beta + Za + \varepsilon, \quad (20)$$

where X and Z are design matrices that define model structure, β is a vector of F fixed effects, a is a vector of E random effects and ε are residuals. Random effects and residuals are assumed to be MVN with zero mean and covariance matrices G and R , respectively. For simplicity we assume that $G = \sigma_a^2 A$, where A is a known symmetric matrix, and $R = \sigma_e^2 I$, where I is the identity matrix (such that residuals are uncorrelated between measurements). $r^2 = \sigma_a^2 / (\sigma_a^2 + \sigma_e^2)$ measures the relative contribution of random effects to residuals.

Speed comparison

We present three example models to illustrate how algorithm performance depends on the nature of the covariance matrix A (a detailed development of PBP proposals for the MM model framework is presented in Appendix L):

Uncorrelated random effects ($A=I$)

Simulated data was generate using $N=10^5$, $E=100$, $F=2$ (see Appendix L for further details). Figure 10(a) shows how the computational time to infer r^2 varies as the value of r^2 used to generate the data changes. The standard Gibbs approach is consistently fastest because here the data is highly informative about the latent variables. Rather than the posterior exhibiting strong correlations between latent variables and parameters (as in Fig. 1(a)), it in fact shows very little correlation. This illustrates that when mixing is good, PBPs are not expected to speed up MCMC.

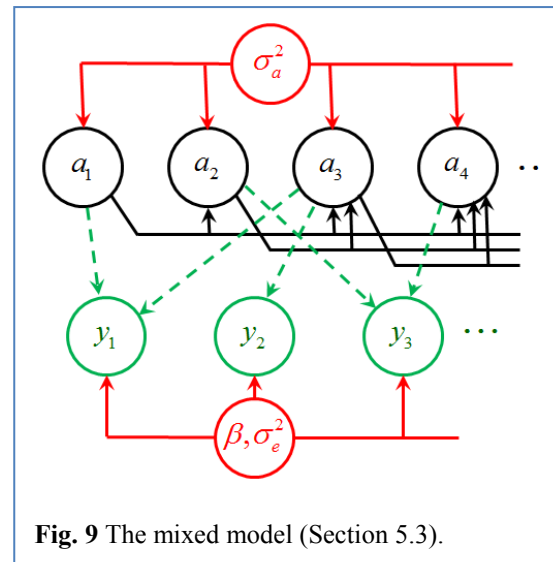


Fig. 9 The mixed model (Section 5.3).

Correlated random effects (A^{-1} sparse)

An important application of mixed models is in the field of quantitative genetics, which aims to understand the genetic basis of traits of interest [30]. As an illustration take y to represent measurements of height within a population. In contrast to the previous example, observations *are* correlated between members in a population, *e.g.* if an individual has tall parents they are more likely to be tall. This correlation results from genetic inheritance. The relatedness of individuals within the population is captured by the so-called “relationship matrix” A .

Simulated data were generated assuming a population randomly mated over four generations with $N=E=4 \times 10^3$, $F=2$ (see Appendix L for further details). Figure 10(b) shows how the computational time to infer r^2 varies with the r^2 value used to generate the data. Disregarding fixed effects, $r^2=0$ implies no genetic inheritance and $r^2=1$ corresponds to a trait dominated by genetic inheritance. In these limits Gibbs sampling slows down significantly due to strong parameter-latent variable correlations in the posterior, leading to poor mixing. Using ID_0 shows an improvement over Gibbs for low r^2 , however for high r^2 its performance proves to be poor. Using ID_1 and ID_2 leads to further improvements in computational speed, resulting in PBPs becoming consistently faster than the standard Gibbs approach (*e.g.*, ID_2 is a factor 100 times faster in the limit $r^2 \rightarrow 0$). The move to ID_3 shows little improvement and for ID_4 , ID_5 *etc.* PBPs become progressively slower despite mixing better. Consequently ID_2 , which uses measurements taken on individuals as well as close relatives, represents an optimum choice in this particular example.

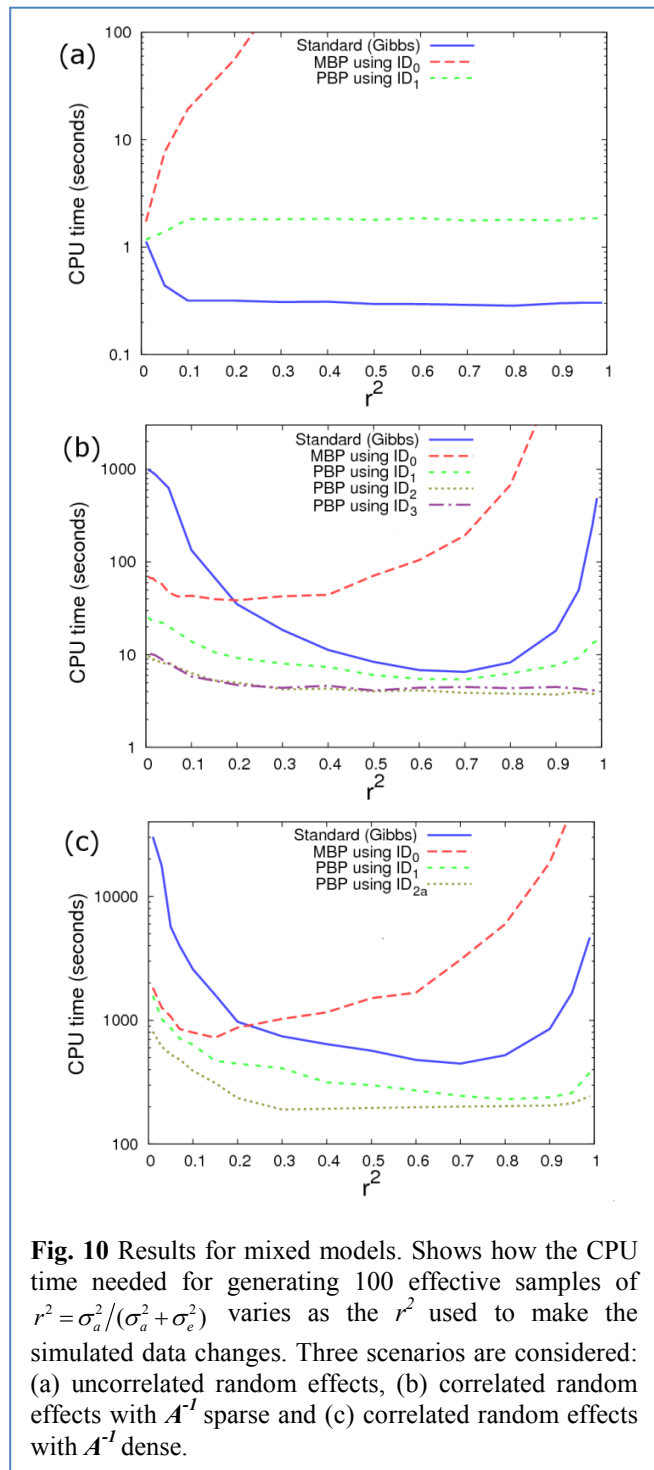


Fig. 10 Results for mixed models. Shows how the CPU time needed for generating 100 effective samples of $r^2 = \sigma_a^2 / (\sigma_a^2 + \sigma_e^2)$ varies as the r^2 used to make the simulated data changes. Three scenarios are considered: (a) uncorrelated random effects, (b) correlated random effects with A^{-1} sparse and (c) correlated random effects with A^{-1} dense.

Correlated random effects (A^{-1} dense)

In cases in which the relationship matrix \mathbf{A} is unknown it can be approximated by the genomic relationship matrix [31] (which is calculated using the measured genotypes of all individuals¹⁴). Such an approach results in all elements in \mathbf{A}^{-1} being non-zero (whereas the vast majority of them were exactly zero before).

We mimic this change by adding small random contributions to \mathbf{A}^{-1} and repeat the previous analysis¹⁵. The results are shown in Fig. 10(c). The general pattern is largely the same as in Fig. 10(b), although all approaches are now considerably slower due to the additional computations necessary. An important point to mention is how ID_{2a} is generated under this scenario. ID_2 ordinarily uses information from all those additive genetic effects that depend on a_e (as well as their predecessors). When \mathbf{A}^{-1} is dense, this approach is extremely slow because of the large number of dependencies within the model. However, huge gains in speed can be achieved by selecting only those dependencies which are deemed large (see Appendix L). This illustrates that ignoring weak dependencies can be an effective general approach to reducing the computational cost associated with calculating IDs.

5.4 Generalized linear mixed models (GLMM)

GLMMs are a widely used extension of MMs that account for non-normally distributed observations [20]. The vector of observations \mathbf{y} is now drawn from

$$\mathbf{y} \sim \chi(\boldsymbol{\mu}), \quad (21)$$

where χ belongs to the exponential family of distributions (which includes the normal, binomial, Poisson and gamma distributions). The vector of means $\boldsymbol{\mu}$ depends on fixed and random effects thorough a link function g

$$\boldsymbol{\mu} = g^{-1}(\mathbf{X}\boldsymbol{\beta} + \mathbf{Z}\mathbf{a}), \quad (22)$$

where \mathbf{X} and \mathbf{Z} are design matrices that define the model structure, $\boldsymbol{\beta}$ is a vector of F fixed effects, and \mathbf{a} is a vector of E random effects (which are assumed to be MVN with zero mean and covariance matrix \mathbf{G}). In contrast to the MM expression in Eq.(20), the residuals $\boldsymbol{\varepsilon}$ no longer appear here as any discrepancies between the data \mathbf{y} and the model are incorporated into χ in Eq.(21).

As an illustrative example of a GLMM, consider data \mathbf{y} consisting of binary (0/1) measurements of disease status (representing uninfected/infected) that are explained in terms of a quantitative genetics model (like the one introduced in Section 5.3). In this case χ is chosen to be a Bernoulli distribution and g is a logit function such that

$$\boldsymbol{\mu} = \frac{1}{1 + e^{-(\mathbf{X}\boldsymbol{\beta} + \mathbf{Z}\mathbf{a})}}. \quad (23)$$

¹⁴ Often this is done by measuring commonly varying bases along the genome called “single nucleotide polymorphisms” (SNPs).

¹⁵ Uniformly randomly selected in the range -0.005 to 0.005.

Although PBPs can be applied in the general case, here we assume one additive genetic effect per individual (*i.e.* $\mathbf{Z}=\mathbf{I}$) and $\mathbf{G} = \sigma_a^2 \mathbf{A}$ (where \mathbf{A} is the relationship matrix). Under this model $\mathbf{x}\boldsymbol{\beta} + \mathbf{a}$ is a vector giving each individual's propensity for disease (which is assumed to be normally distributed) and \mathbf{a} represents the additive genetic component of this quantity. Appendix M provides further details.

Speed comparison

For GLMMs Gibbs sampling is no longer possible, so instead a standard random walk MH scheme is implemented. Furthermore, since the model no longer contains parameter σ_e^2 (because no such parameter exists for the Bernoulli distribution), σ_a^2 is used to quantify the relative importance of genetics to an individual's propensity for disease.

We again assume a population of individuals randomly mated over four generations with $N=E=4\times 10^3$, $F=2$ (see Appendix M for further details). Figure 11 shows how the computational time to infer σ_a^2 varies with the value of σ_a^2 used to generate the data. We see that algorithm speeds are considerably slower than for the corresponding MM containing the same number of individuals (Fig. 10(b)). This is because the information contained within the observations (*i.e.* binary disease measurements) is significantly less than when traits are measured directly (*e.g.* as for quantitative measurements such as height), resulting in greater uncertainty in the underlying additive genetic effects and consequently a larger posterior parameter space.

Figure 11 shows that PBPs using ID_1 (which represent the optimum algorithm in this particular case) are consistently faster than the standard MCMC by a factor of around 30 (roughly independent of the value of σ_a^2).

6 Summary

This paper introduced posterior-based proposals (PBP) and demonstrated that they speed up MCMC inference in many cases where existing approaches perform poorly. PBP are applicable to the majority of statistical models (namely, those whose conditional dependence structure is expressible in terms of a directed acyclic graph) [32]. Performance is enhanced by improving mixing of MCMC (*i.e.* increasing the rate at which they generate uncorrelated samples) by jointly proposing changes to model parameters θ and latent variables ξ (see Section 3 for details). PBPs are a family of proposal schemes built by generating importance distributions (ID_0 , ID_1 , *etc.*) that systematically account for dependence structure in the Bayesian posterior with increasing accuracy. The zeroth-order approximation ID_0 ignores the data and thus corresponds to "model-based proposals" (MBPs) [10]. The optimal level of approximation depends on problem specific trade-offs between improved

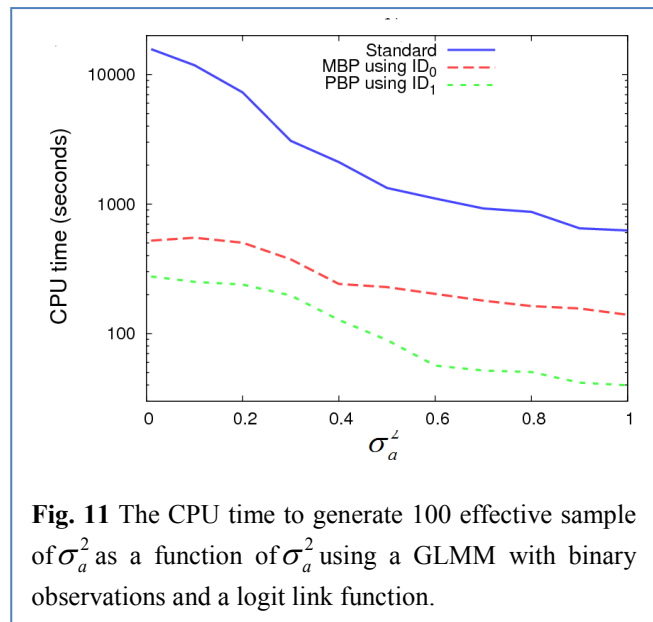


Fig. 11 The CPU time to generate 100 effective sample of σ_a^2 as a function of σ_a^2 using a GLMM with binary observations and a logit link function.

mixing resulting from increased acceptance rates and the computational cost of generating suitably accurate IDs.

The relative computational speed of PBP MCMC compared to “standard” Gibbs/random walk MH techniques was investigated for benchmark models used in applications ranging from finance to ecology to statistical genetics. Unsurprisingly in cases where mixing of the MCMC chain is not an issue for standard approaches, PBPs were not significantly faster (indeed for a mixed model with uncorrelated random effects Gibbs sampling was actually found to be faster). However, in many scientifically challenging applications such correlations are critical, *e.g.* in quantitative genetics where they represent relatedness between individuals [19], and in such cases PBPs were found to be substantially faster than Gibbs sampling. This was especially true when inferring the size of small random effects (corresponding to traits with only a small component of genetic inheritance [33, 34]), where performance was up to two orders of magnitude faster.

7 Discussion

We now discuss PBPs in relation to two widely used techniques for overcoming slow mixing: PMCMC and HMCMC.

As stated previously, PMCMC only works on problems in which data can be incorporated in a sequential manner (*i.e.* it would not be suitable for the examples in Sections 5.1, 5.3 and 5.4 above). Even then, however, PMCMC can become slow due to requiring a very large number of particles to give a reasonable acceptance rate¹⁶. Indeed, a previous paper [10] using observations taken from multiple spatially linked epidemics showed that PMCMC became much slower in comparison to an MBP approach as the number of epidemics was increased. However, a key advantage of PMCMC approaches is that they are usually relatively easy to implement and typically allow for efficient parallelization.

HMCMC relies on calculating gradients in the log-likelihood, and hence is not applicable to models with discrete variables (*e.g.* the example in Section 5.1) or when the number of variables within the model changes. Its efficiency is very much dependent on the shape of the posterior. Often it is tested on high dimensional multivariate normal-type posterior distributions, where it is found to perform well against other approaches [4]. However in many real world problems there can be sharp gradients in which some parameters change much more rapidly than others. These irregularities necessitate lots of small intermediary steps for each MCMC iteration, significantly reducing its performance. In contrast to PMCMC, HMCMC cannot easily be parallelised.

Finally we come to PBPs introduced here. Generally speaking they tend to work better (in comparison to both standard approaches and HMCMC) on problems which are “model dominant”. By this we mean that the shape of the posterior is largely represented by the latent process likelihood, with the observation model providing a small perturbation on top of this. A good example of this would be a complex model applied to relatively few actual measurements. (Note, PMCMC also works well under such scenarios because fewer particles are required for a reasonable

¹⁶ This happens in cases in which after simulating between successive time points the probability of the observed data is small, either because the observations themselves are very specific, or because multiple measurements are made.

acceptance rate.) The reason that both PMCMC and PBPs work in this model dominant regime can be seen if we look at the limiting case in which there is no data. Here both methods easily map out the prior distribution for model parameters (with latent variables naturally being dealt with by simulation in the former and MBPs in the latter). In contrast HMCMC is faced with the potentially difficult task of integrating from one parameter / latent variable combination to another, often taking a large number of steps to do so. The flip side of this argument, however, is the “data dominant” regime, in which there is a lot of data and a relatively simple model. In this case we might naturally expect HMCMC to work better than either PMCMC or PBPs. However, here mixing itself is typically fast and so standard approaches would usually suffice. Like HMCMC, PBPs also cannot easily be parallelised. However a potential extension to PBPs would be to incorporate them into a particle-like framework in which multiple proposals are made along with a particle filter applied at different time points. This may lead to further improvements in speed under some scenarios, and will be the subject of future investigation.

One final point to mention is that whilst some complex models may not fit into the DAG structure required by PBPs, it may be that certain subsections of them do. Here PBPs could still profitably be used by fixing all non-DAG elements of the model under the proposal (whereby they are incorporated into the data y for the purposes of the proposal step). Whatever the complexity of the model, therefore, PBPs can be considered as an additional tool in the MCMC programmer’s arsenal.

Appendices

Appendix A: Importance sampling

Importance sampling (IS) is a general technique for estimating properties of a given distribution (which can't directly be sampled from) using samples generated from a different (more accessible) distribution [35, 36]. We emphasise that PBPs are *not* a type of IS, but do make use of importance distributions (IDs). Therefore a brief description is now given. The posterior in Eq.(1) can be expressed as

$$\pi(\theta, \xi | y) = \pi(\xi | \theta, y) \pi(\theta | y), \quad (24)$$

which, using Eq.(2), may be written

$$\pi(\theta, \xi | y) = \pi(\theta | y) \prod_{e=1}^E \pi(\xi_e | \xi_{e' < e}, \theta, y). \quad (25)$$

This implies that, in principle, posterior samples can be generated by first sampling θ from $\pi(\theta | y)$, then ξ_1 from $\pi(\xi_1 | \theta, y)$, then ξ_2 from $\pi(\xi_2 | \xi_1, \theta, y)$, and so on and so forth until a complete set of latent variables ξ is generated. Unfortunately, however, these distributions are typically intractable, so cannot be directly sampled. To overcome this difficulty importance distributions (IDs) $f_{ID}(\theta | y)$ (which, for example, could be chosen to be multivariate normal) and $f_{ID}(\xi_e | \xi_{e' < e}, \theta, y)$ (a set of univariate distributions, such as normal or Poisson, for each variable e) are defined which *can* be sampled from. IDs are chosen to resemble the true distributions as closely as possible.

IS consists of first sampling θ from $f_{ID}(\theta | y)$ and then successively drawing ξ_e from $f_{ID}(\xi_e | \xi_{e' < e}, \theta, y)$ for $e=1$ to E . The resulting sample θ, ξ has an associated “weight”

$$w = \frac{\pi(y | \xi, \theta) \pi(\xi | \theta) \pi(\theta)}{f_{ID}(\theta | y) \prod_{e=1}^E f_{ID}(\xi_e | \xi_{e' < e}, \theta, y)}, \quad (26)$$

which accounts for the fact that it isn't a true posterior sample [35]. Repeating IS a sufficient number of times gives unbiased estimates for posterior quantities of interest. For example, if i indexes sample number then

$$\langle \theta \rangle = \sum_i \theta^i w^i / \sum_i w^i \quad (27)$$

gives an estimate for parameter posterior means¹⁷. Unfortunately IS becomes highly inefficient for complex models because the vast majority of samples have negligible weight (leading to poor statistical estimates for quantities such as those in Eq.(27)). This necessitates the use of MCMC approaches in the first place.

In summary, this appendix has identified importance distributions $f_{ID}(\xi_e | \xi_{e' < e}, \theta, y)$ (which take standard functional forms such as normal, Poisson, *etc.*) that aim to account for both the model and observations by approximating $\pi(\xi_e | \xi_{e' < e}, \theta, y)$. For example supposing that $\pi(\xi_e | \xi_{e' < e}, \theta, y)$ has a

¹⁷ The average of the weights themselves $\sum_i w^i / N$ gives an unbiased estimate of the model evidence $\pi(y)$.

normal-like distribution, the importance distribution would be chosen to be normal¹⁸ $f_{ID}(\xi_e | \xi_{e' < e}, \theta, y) = f_{\text{norm}}(\xi_e | \mu(\xi_{e' < e}, \theta, y), \sigma(\xi_{e' < e}, \theta, y))$ with mean μ and standard deviation σ functionally depend on $\xi_{e' < e}$, θ and y . Details on these functional dependencies are given in Section 4.

Appendix B: Derivation of PBP for Poisson or normal IDs

Here we explicitly demonstrate the validity of the two conditions in Eq.(6) when using the sampling procedures outlined in Table 1 for the Poisson and normal IDs.

Poisson ID

For a model which utilises a Poisson ID for latent variable ξ_e , the following probability mass functions are defined:

$$\begin{aligned} f_{ID}(\xi_e^i | \xi_{e' < e}^i, \theta^i, y) &= \frac{\lambda_i^{\xi_e^i} e^{-\lambda_i}}{\xi_e^i!}, \\ f_{ID}(\xi_e^p | \xi_{e' < e}^p, \theta^p, y) &= \frac{\lambda_p^{\xi_e^p} e^{-\lambda_p}}{\xi_e^p!}, \end{aligned} \tag{A1}$$

where λ_i is some known function of $(\xi_{e' < e}^i, \theta^i, y)$ and λ_p is some known function of $(\xi_{e' < e}^p, \theta^p, y)$.

Suppose, arbitrarily, that the expected number of occurrences in the proposed state λ_p is greater than the expected number in the initial state λ_i . Table 1 shows that the actual number in the proposed state ξ_e^p is calculated using

$$\xi_e^p = \xi_e^i + X, \tag{A2}$$

where ξ_e^i is the number in the initial state and X is sampled from a Poisson distribution with average number given by the difference between λ_p and λ_i :

$$X \sim \text{Pois}(\lambda_p - \lambda_i). \tag{A3}$$

The probability of this proposal is given by

$$g(\xi_e^p) = \frac{(\lambda_p - \lambda_i)^{\xi_e^p - \xi_e^i} e^{-(\lambda_p - \lambda_i)}}{(\xi_e^p - \xi_e^i)!}. \tag{A4}$$

Interchanging i and p in Table 1 shows that the reverse transition is taken from a binomial probability distribution

$$\xi_e^i \sim B(\xi_e^p, \frac{\lambda_i}{\lambda_p}), \tag{A5}$$

with proposal probability

¹⁸ See Appendix G for a definition of this distribution.

$$g(\xi_e^i) = \frac{\xi_e^p!}{\xi_e^i!(\xi_e^p - \xi_e^i)!} \left(\frac{\lambda_i}{\lambda_p}\right)^{\xi_e^i} \left(1 - \frac{\lambda_i}{\lambda_p}\right)^{\xi_e^p - \xi_e^i}. \quad (\text{A6})$$

Combining the results from Eqs.(A4) and (A6) gives

$$\begin{aligned} \frac{g(\xi_e^i)}{g(\xi_e^p)} &= \frac{\xi_e^p!}{\xi_e^i!(\xi_e^p - \xi_e^i)!} \left(\frac{\lambda_i}{\lambda_p}\right)^{\xi_e^i} \left(1 - \frac{\lambda_i}{\lambda_p}\right)^{\xi_e^p - \xi_e^i} \times \left(\frac{\left(\lambda_p - \lambda_i\right)^{\xi_e^p - \xi_e^i} e^{-(\lambda_p - \lambda_i)}}{(\xi_e^p - \xi_e^i)!} \right)^{-1} \\ &= \frac{\lambda_p^{\xi_e^i} e^{-\lambda_i}}{\xi_e^i!} \times \left(\frac{\lambda_p^{\xi_e^p} e^{-\lambda_p}}{\xi_e^p!} \right)^{-1}. \end{aligned} \quad (\text{A7})$$

Using this, along with Eq.(A1), finally gives

$$\frac{f_{ID}(\xi_e^p | \xi_{e' < e}^p, \theta^p, y)}{f_{ID}(\xi_e^i | \xi_{e' < e}^i, \theta^i, y)} \frac{g(\xi_e^i)}{g(\xi_e^p)} = \frac{\lambda_p^{\xi_e^p} e^{-\lambda_p}}{\xi_e^p!} \left(\frac{\lambda_i^{\xi_e^i} e^{-\lambda_i}}{\xi_e^i!} \right)^{-1} \frac{\lambda_p^{\xi_e^i} e^{-\lambda_i}}{\xi_e^i!} \left(\frac{\lambda_p^{\xi_e^p} e^{-\lambda_p}}{\xi_e^p!} \right)^{-1} = 1, \quad (\text{A8})$$

which shows that condition 1 in Eq.(6) is, indeed, satisfied. Condition 2 is satisfied because $X=0$ when $\lambda_p = \lambda_i$ in Eq.(A3), and so by definition $\xi^p = \xi^i$ in Eq.(A2).

Normal ID

Here we consider the case of a normal ID for latent variable ξ_e :

$$\begin{aligned} f_{ID}(\xi_e^i | \xi_{e' < e}^i, \theta^i, y) &= \frac{1}{\sqrt{2\pi}\sigma_i} e^{-\frac{(\xi_e^i - \mu_i)^2}{2\sigma_i^2}}, \\ f_{ID}(\xi_e^p | \xi_{e' < e}^p, \theta^p, y) &= \frac{1}{\sqrt{2\pi}\sigma_p} e^{-\frac{(\xi_e^p - \mu_p)^2}{2\sigma_p^2}}. \end{aligned} \quad (\text{A9})$$

Suppose, arbitrarily, that the standard deviation in the proposed state σ_p is smaller than in the initial state σ_i . Table 1 shows that the proposal for ξ_e^p is given by

$$\xi_e^p \sim N\left(\mu_p + \alpha \frac{\sigma_p^2}{\sigma_i^2} (\xi_e^i - \mu_i), \kappa \frac{\sigma_p^2}{\sigma_i^2} (\sigma_i^2 - \sigma_p^2)\right), \quad (\text{A10})$$

where $\alpha^2 = \kappa + (1 - \kappa) \frac{\sigma_i^2}{\sigma_p^2}$ and κ is a tuneable constant. The probability density function for generating this final state is given by

$$g(\xi_e^p) = \frac{1}{\sqrt{2\pi\kappa \frac{\sigma_p^2}{\sigma_i^2} (\sigma_i^2 - \sigma_p^2)}} e^{-\frac{\left(\xi_e^p - \left(\mu_p + \alpha \frac{\sigma_p^2}{\sigma_i^2} (\xi_e^i - \mu_i)\right)\right)^2}{2\kappa \frac{\sigma_p^2}{\sigma_i^2} (\sigma_i^2 - \sigma_p^2)}}. \quad (\text{A11})$$

We now consider the reverse transition. Since p and i are now switched in Table 1, the corresponding proposal probability density function is given by

$$g(\xi_e^i) = \frac{1}{\sqrt{2\pi\kappa(\sigma_i^2 - \sigma_p^2)}} e^{-\frac{(\xi_e^i - \mu_i + \alpha(\xi_e^p - \mu_p))^2}{2\kappa(\sigma_i^2 - \sigma_p^2)}}. \quad (\text{A12})$$

The ratio between Eqs.(A12) and (A11) is given by

$$\begin{aligned} \frac{g(\xi_e^i)}{g(\xi_e^p)} &= \sqrt{\frac{\sigma_p^2}{\sigma_i^2}} e^{-\frac{1}{2\kappa(\sigma_i^2 - \sigma_p^2)} \left[\left((\xi_e^i - \mu_i) - \alpha(\xi_e^p - \mu_p) \right)^2 - \frac{\sigma_i^2}{\sigma_p^2} \left((\xi_e^p - \mu_p) - \alpha \frac{\sigma_p^2}{\sigma_i^2} (\xi_e^i - \mu_i) \right)^2 \right]} \\ &= \sqrt{\frac{\sigma_p^2}{\sigma_i^2}} e^{-\frac{1}{2\kappa(\sigma_i^2 - \sigma_p^2)} \left[(\xi_e^i - \mu_i)^2 + \alpha^2 (\xi_e^p - \mu_p)^2 - 2\alpha (\xi_e^i - \mu_i) (\xi_e^p - \mu_p) - \left(\frac{\sigma_i^2}{\sigma_p^2} (\xi_e^p - \mu_p)^2 + \alpha^2 \frac{\sigma_p^2}{\sigma_i^2} (\xi_e^i - \mu_i)^2 - 2\alpha (\xi_e^p - \mu_p) (\xi_e^i - \mu_i) \right) \right]} \\ &= \sqrt{\frac{\sigma_p^2}{\sigma_i^2}} e^{-\frac{1}{2\kappa(\sigma_i^2 - \sigma_p^2)} \left[\left(1 - \alpha^2 \frac{\sigma_p^2}{\sigma_i^2} \right) (\xi_e^i - \mu_i)^2 + \left(\alpha^2 - \frac{\sigma_i^2}{\sigma_p^2} \right) (\xi_e^p - \mu_p)^2 \right]} \\ &= \sqrt{\frac{\sigma_p^2}{\sigma_i^2}} e^{-\frac{\sigma_i^2 - \alpha^2 \sigma_p^2}{2\kappa(\sigma_i^2 - \sigma_p^2)} \left[\frac{1}{\sigma_i^2} (\xi_e^i - \mu_i)^2 - \frac{1}{\sigma_p^2} (\xi_e^p - \mu_p)^2 \right]}. \end{aligned} \quad (\text{A13})$$

The definition $\alpha^2 = \kappa + (1 - \kappa) \frac{\sigma_i^2}{\sigma_p^2}$ can be rearrange to $\kappa(\sigma_i^2 - \sigma_p^2) = \sigma_i^2 - \alpha^2 \sigma_p^2$, leading to

$$\begin{aligned} \frac{g(\xi_e^i)}{g(\xi_e^p)} &= \sqrt{\frac{\sigma_p^2}{\sigma_i^2}} e^{-\frac{\sigma_i^2 - \alpha^2 \sigma_p^2}{2\kappa(\sigma_i^2 - \sigma_p^2)} \left[\frac{1}{\sigma_i^2} (\xi_e^i - \mu_i)^2 - \frac{1}{\sigma_p^2} (\xi_e^p - \mu_p)^2 \right]} \\ &= \frac{1}{\sqrt{2\pi\sigma_i^2}} \left(e^{-\frac{1}{2\sigma_i^2} (\xi_e^i - \mu_i)^2} \right) \left[\frac{1}{\sqrt{2\pi\sigma_p^2}} \left(e^{-\frac{1}{2\sigma_p^2} (\xi_e^p - \mu_p)^2} \right) \right]^{-1}. \end{aligned} \quad (\text{A14})$$

This, together with the expressions in Eq.(A9), shows that condition 1 in Eq.(6) is, indeed, satisfied. Furthermore, condition 2 is satisfied by noting that the variance in the proposal in Eq.(A10) goes to zero when $\sigma_p^2 = \sigma_i^2$.

The validity of all the sampling procedures in Table 1 can be verified by following essentially the same procedure as above to show that the two conditions in Eq.(6) are satisfied.

Appendix C: Adaptation period

Posterior-based proposals contain two quantities in Eq.(8) that need to be established: a numerical approximation to the covariance matrix of the posterior Σ^θ , and a jumping size j . Motivated by adaptive MCMC [37, 38], these are calculated during an ‘‘adaptation’’ period, which also acts as the required burn-in phase (*i.e.* this ensures that the first sample drawn after the adaptation period is

representative of a random draw from the posterior). In this study $I^{ad}=10^4$ iterations are used for adaptation, and subsequently Σ^θ and j are fixed¹⁹.

Covariance matrix Σ_θ : During the adaptation period the number of MCMC iterations i changes from 1 to I^{ad} . An approximation to the posterior covariance matrix Σ^θ is calculated every 100 iterations based on samples from $i/2$ to i :

$$\Sigma_{mn}^\theta = \frac{1}{\frac{1}{2}i - 1} \sum_{i'=\frac{i}{2}}^i (\theta_m^{i'} - \bar{\theta}_m)(\theta_n^{i'} - \bar{\theta}_n), \quad \bar{\theta}_m = \frac{1}{\frac{1}{2}i} \sum_{i'=\frac{i}{2}}^i \theta_m^{i'}. \quad (B1)$$

This is effectively equivalent to using a dynamically changing burn-in period set at half the current iteration number. As the adaptation period progresses the estimated covariance matrix Σ^θ becomes a better and better approximation, which helps to improve the efficiency of the algorithm. For the first 100 samples Σ^θ is set to a diagonal matrix with elements chosen to be sufficiently small to ensure a good initial acceptance rate.

Jumping size j : This determines the acceptance rate for PBPs in Eq.(9). If j is too large very few proposals are accepted, and if too small mixing is slow. A robust heuristic method for optimising j is as follows. Initially j is set to a small quantity. Each time a PBP is accepted, j is updated according to

$$j^{new} = j \times 1.02, \quad (B2)$$

and when rejected

$$j^{new} = j \times 0.99. \quad (B3)$$

These numerical factors are chosen for two reasons: Firstly, the two updates in Eqs.(B2) and (B3) balance each other out when acceptance occurs around 33% of the time (which from Appendix H was found to be approximately optimal), leading to a steady state solution for j . Secondly, they are sufficiently close to 1 to prevent large fluctuations in j , but sufficiently far to allow for the steady state solution to be found during the adaptation period.

Appendix D: Derivation of acceptance probability

We derive the expression in Eq.(9). Based on Eq.(1), the MH acceptance probability is given by

$$P_{MH} = \min \left\{ 1, \frac{\pi(y|\xi^p, \theta^p) \pi(\xi^p|\theta^p) \pi(\theta^p)}{\pi(y|\xi^i, \theta^i) \pi(\xi^i|\theta^i) \pi(\theta^i)} \frac{g^{p \rightarrow i}}{g^{i \rightarrow p}} \right\}, \quad (C1)$$

where $g^{i \rightarrow p}$ represents the proposal probability density for generating θ^p and ξ^p given the current state θ^i and ξ^i , and $g^{p \rightarrow i}$ represents the corresponding quantity in the opposite direction²⁰. Following steps 1 and 2 in the PBP algorithm from Section 3.4, the overall proposal probability can be expressed as

$$g^{i \rightarrow p} = f_{MVN}(\theta^p - \theta^i, j^2 \Sigma^\theta) \prod_{e=1}^E g(\xi_e^p). \quad (C2)$$

¹⁹ This ensures that detailed balance is strictly enforced when MCMC samples are actually taken.

²⁰ In other words, starting at θ^p and ξ^p and proposing the state θ^i and ξ^i .

Substituting this, along with the reverse transition, into Eq.(C1) (and noting that the MVN distributions are symmetric²¹), gives

$$P_{MH} = \min \left\{ 1, \frac{\pi(y|\xi^p, \theta^p) \pi(\xi^p|\theta^p) \pi(\theta^p)}{\pi(y|\xi^i, \theta^i) \pi(\xi^i|\theta^i) \pi(\theta^i)} \prod_{e=1}^E \frac{g(\xi_e^p)}{g(\xi_e^i)} \right\}. \quad (C3)$$

Substituting condition 1 from Eq.(6) into this expression leads to the final result in Eq.(9).

Appendix E: Further insights into PBPs

Here we provide some additional notes on the PBP algorithm in Section 3.4:

Step 1: Strong posterior correlations can exist not only between model parameters and latent variables (as demonstrated in Fig. 1(a)), but also between different model parameters themselves (*i.e.* after marginalisation over latent variables). Equation (8) helps to mitigate against these, helping to further facilitating mixing. Other possibilities for proposals in parameter space are discussed in Appendix F (along with complications such as what to do when parameters are discrete rather than continuous) and sampling from MVNs using Cholesky decomposition [39] is described in Appendix G.

Step 2: This step makes use of IDs $f_{ID}(\xi_e | \xi_{e' < e}, \theta, y)$, which approximate the univariate distributions $\pi(\xi_e | \xi_{e' < e}, \theta, y)$ for $e=1, \dots, E$ (with functional form chosen to provide good approximation to the model under study). Each functional form for the IDs is associated with a different (posterior based) proposal distributions $g(\xi_e^p)$ satisfying Eq.(6) (see Table 1). IDs are characterised by one or two parameters (*e.g.* an expected event number in the Poisson case and a mean and variance in the normal case) and for $e > 1$ these functionally depend on latent variables with lower index (as determined by the DAG structure of the underlying the model) and the model parameters and data.

Step 3: Two limiting cases in Eq.(9) are of particular importance. Firstly, as $f_{ID}(\xi_e | \xi_{e' < e}, \theta, y)$ becomes more and more representative of $\pi(\xi_e | \xi_{e' < e}, \theta, y)$, the MH probability reduces to

$$P_{MH} = \min \left\{ 1, \frac{\pi(\theta^p|y)}{\pi(\theta^i|y)} \right\}. \quad (D1)$$

The originally high dimensional problem (containing latent variables ξ and parameters θ) is reduced to a much lower dimensional problem (containing just the parameters θ), helping explain why mixing is potentially so much faster.

Secondly, as the jumping size in parameter space gets smaller (as determined by j in Eq.(8)) so $P_{MH} \rightarrow 1$. This is of particular importance because it means that even if the IDs provide a relatively poor approximation to $\pi(\xi_e | \xi_{e' < e}, \theta, y)$, provided j is made sufficiently small a substantial fraction of proposals will always be accepted. In practice the jumping size j is optimally tuned to ensure acceptance around 33% of the time (see Appendix C for details).

Appendix F: Other possibilities for proposals in parameter space

Three issues are discussed in relation to proposals in parameter space:

²¹ The probability of jumping from θ^i to θ^p is the same as from θ^p to θ^i .

1) Optimisation

The proposal distribution in parameter space introduced in Eq.(8) has the advantage of being simple and robust against highly correlated model parameters. Generally speaking, however, it may not represent the optimum choice. For example, if two variables A and B are largely uncorrelated in the posterior it may actually be computationally faster to consider proposals to A and B separately. This is especially true in cases when proposing changes to A is much faster (*e.g.* fixed effects in mixed models) than B (*e.g.* random effects).

In the most general case, a combination of the following two types of proposal can be used in Eq.(8):

Single parameters changes – A single parameter k is selected from θ . θ_k^p is then sampled from a simple normal distribution centred at θ_k^i :

$$\theta_k^p \sim N(\theta_k^i, \sigma_k^2), \quad \theta_{l \neq k}^p = \theta_l^i. \quad (\text{E1})$$

Multiple parameter changes – χ represent a subset of the parameters in θ , and θ_χ^p is sampled from a multivariate normal distribution centred at θ_χ^i :

$$\theta_\chi^p \sim N(\theta_\chi^i, j_\chi^2 \Sigma^\chi), \quad \theta_{l \notin \chi}^p = \theta_l^i. \quad (\text{E2})$$

Providing an automated way to determine the optimum choice for proposals in parameter space for a given model will be the subject of future research.

2) Parameters not continuous

In some cases model parameters are discrete, *e.g.* for an epidemiological model the initial population numbers in various compartments might be included in θ . If these discrete variables are approximately normally distributed (as they would be if the population sizes are reasonably large), then we could again draw a vector v from a MVN distribution as before

$$v \sim N(\theta^i, j^2 \Sigma^\theta), \quad (\text{E3})$$

but this time round those discrete model variables to the nearest integer

$$\theta_k^p = \begin{cases} \text{round}(v_j), & \text{if } \theta_j \text{ discrete} \\ v_j, & \text{if } \theta_j \text{ continuous} \end{cases} \quad (\text{E4})$$

In cases in which model parameters are not expected to be approximately normally distributed they can simply be updated individually.

3) Restrictions

For some of the functional forms in Table 1, only one of the characteristic parameters can be updated at a time. For example, for the beta distribution only α can be changed whilst fixing β , or *vice versa*. Consequently, proposals to both α and β cannot be performed simultaneously.

Appendix G: Normal distributions

The probability density function for drawing a value x from a normal distribution with mean μ and variance σ^2 is given by

$$f_{\text{norm}}(x | \mu, \sigma^2) = \frac{1}{\sqrt{2\pi\sigma^2}} e^{-\frac{(x-\mu)^2}{2\sigma^2}}. \quad (\text{F1})$$

The equivalent multivariate normal distribution is

$$f_{\text{MVN}}(\mathbf{x} | \boldsymbol{\mu}, \boldsymbol{\Sigma}) = \frac{1}{\sqrt{(2\pi)^d |\boldsymbol{\Sigma}|}} e^{-\frac{1}{2}(\mathbf{x}-\boldsymbol{\mu})^T \boldsymbol{\Sigma}^{-1}(\mathbf{x}-\boldsymbol{\mu})}, \quad (\text{F2})$$

where d is the number of dimensions and $\boldsymbol{\Sigma}$ is the covariance matrix that captures the variance of individual elements (e.g. parameters) as well as covariance between them.

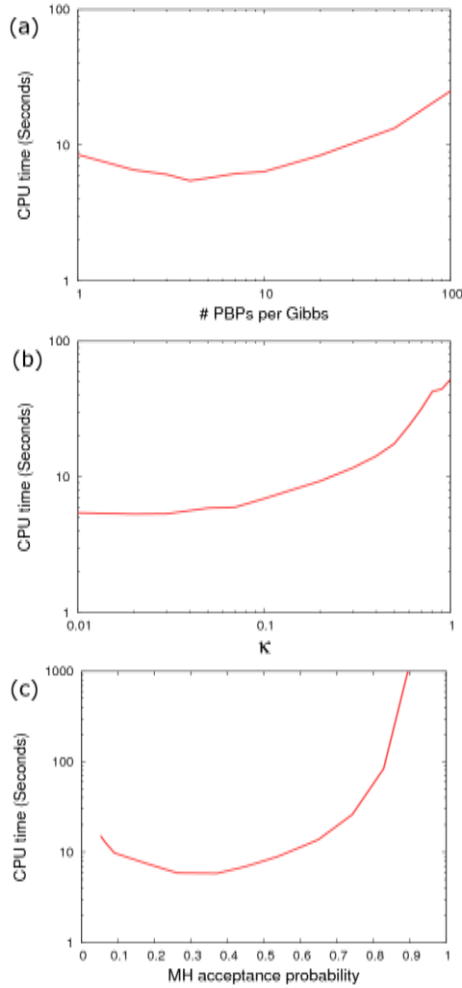


Figure H: Optimisation of key parameters.

that this particular curve has a minimum at $U=4$ updates, although computation speed is found to not be particularly sensitive to its exact value.

Cholesky decomposition provides a standard way to draw samples from a multivariate normal distribution [39]. Provided $\boldsymbol{\Sigma}$ is positive-definite it can be written as $\boldsymbol{\Sigma}=\mathbf{B}\mathbf{B}^T$, where \mathbf{B} is a lower triangular matrix. Samples from the multivariate normal are then generated using

$$\mathbf{x} = \boldsymbol{\mu} + \mathbf{B}\mathbf{z},$$

where \mathbf{z} is a vector of normally distributed independent samples with mean zero and unit variance.

Appendix H: Optimisation of the PBP MCMC algorithm

Figure H illustrates how the PBP algorithm is typically optimised. These results are based on the mixed model applied to quantitative genetics introduced in Section 5.3, but the general findings are found to be largely independent of model type. Optimisation can be considered from three points of view:

Firstly, Fig. H(a) shows the CPU time to generate 100 effective samples of r^2 from the posterior as a function of the number of PBPs between each Gibbs update of the latent variables. We find

Secondly, Fig. H(b) shows variation in CPU time as a function of the tuneable constant κ (this is used in Table 1 in cases in which the ID is normally distributed). Again, performance is largely the same provided κ is smaller than around 0.1. For this study $\kappa=0.03$ was selected.

Finally, Fig. H(c) shows that the algorithm is optimised when the MH acceptance probability is around 33%. This is implemented using the methods outlined in Appendix C.

Appendix I: Effective sample number

Given X correlated MCMC samples of some quantity x^i , the autocorrelation function can be approximated by

$$F_\tau = \frac{1}{(X-\tau)\sigma_x^2} \sum_{i=1}^{X-\tau} (x^i - \bar{x})(x^{i+\tau} - \bar{x}), \quad (\text{H1})$$

where estimates for the average and variance of x are given by

$$\bar{x} = \frac{1}{X} \sum_{i=1}^X x^i, \quad \sigma_x^2 = \frac{1}{X-1} \sum_{i=1}^X (x^i - \bar{x})^2. \quad (\text{H2})$$

The effective sample size is given by the actual sample number X , correcting for correlations between successive samples:

$$X_{eff} = \frac{X}{1 + 2 \sum_{\tau=1}^{\infty} F_\tau}. \quad (\text{H3})$$

When actually calculating X_{eff} , clearly the sum in Eq.(H3) cannot go to infinity. In fact, F_τ often exhibits considerable fluctuations for large τ , and these can generate unwanted bias. The simplest way to deal with these is to truncate the sum in Eq.(H3) up to a maximum size τ_{max} , which is defined to be the largest value of τ for which the following condition holds true (see [40]):

$$F_\tau > 0. \quad (\text{H4})$$

This represents the point at which the autocorrelation function intersects the x -axis.

Appendix J: Details for disease prevalence model

In this appendix we provide additional details relevant to the disease prevalence and diagnostic test model in Section 5.1.

Simulation and prior details

Simulated data was created using $Se_1=Se_2=0.6$ and $Sp_1=Sp_2=0.9$ for $P=1000$ individuals. Different values of the disease prevalence p_D were used to generate Fig. 6(b). The prior distributions for parameters were assumed to be uniform between 0 and 1.

Observation model and latent process likelihood

The model is illustrated in Fig. 5. The true disease status of individuals is represented by Bernoulli variables D_e , where $D_e=1$ (or 0) denotes that individual e is infected (or uninfected) with probability p_D (or $1-p_D$). The test data y_e^t for test type t are 1 (or 0), indicating a positive (or negative) result.

We identify the following model parameters $\theta=\{p_D, Se_1, Sp_1, Se_2, Sp_2\}$ and latent variables $\xi=\{D\}$. The observation model and latent process likelihood are given by

$$\begin{aligned}\pi(y|\xi, \theta) &= \prod_{t=1,2} Se_t^{N_t^{11}} (1-Se_t)^{N_t^{01}} Sp_t^{N_t^{00}} (1-Sp_t)^{N_t^{10}}, \\ \pi(\xi|\theta) &= p_D^{N^1} (1-p_D)^{N^0},\end{aligned}\tag{11}$$

where N^d is the number of individuals with disease status d and N_t^{rd} is the number of cases in which test t gives result r for individuals with disease status d .

Importance distributions

Step 2 of the PBP algorithm (introduced in the Section 3.4) makes use of IDs. Successive approximations for these IDs were then discussed in Section 4. Here we explicitly present expressions for this particular model.

ID₀ is given by the model itself

$$f_{ID_0}(D_e | D_{e'<e}, \theta) = f_{Bern}(D_e | p_D),\tag{12}$$

where f_{Bern} is the Bernoulli probability distribution.

ID₁ takes into account both the model and the observations. From Eq.(16) this is given by

$$f_{ID_1}(D_e | D_{e'<e}, \theta, y) = c f_{Bern}(D_e | p_D) \times \prod_{t=1,2} \pi(y_e^t | D_e),\tag{13}$$

where c is a normalisation constant. Explicitly incorporating the observation model from Eq.(11), this becomes

$$f_{ID_1}(D_e | D_{e'<e}, \theta, y) = f_{Bern}(D_e | \frac{p_1}{p_1+p_0}),\tag{14}$$

where

$$\begin{aligned}p_1 &= p_D \times \begin{cases} Se_1 & \text{if obs. 1 +ve} \\ 1-Se_1 & \text{if obs. 1 -ve} \end{cases} \times \begin{cases} Se_2 & \text{if obs. 2 +ve} \\ 1-Se_2 & \text{if obs. 2 -ve} \end{cases} \\ p_0 &= (1-p_D) \times \begin{cases} 1-Sp_1 & \text{if obs. 1 +ve} \\ Sp_1 & \text{if obs. 1 -ve} \end{cases} \times \begin{cases} 1-Sp_2 & \text{if obs. 2 +ve} \\ Sp_2 & \text{if obs. 2 -ve} \end{cases}.\end{aligned}\tag{15}$$

Since ID₁ actually represent the exact importance distribution, no higher order terms need to be considered in this particular example.

Proposals

As an illustration of how PBPs are implemented in practice, we explicitly go through step 2 of the PBP algorithm from Section 3.4 (which stochastically modifies D_e^i to generate D_e^p).

The ID is given by a Bernoulli distribution with disease probability z :

$$f_{ID}(D_e | D_{e' < e}, \theta, y) = f_{Bern}(D_e | z). \quad (16)$$

For ID_0 , z is equal to p_D and for ID_1 , $z = p_1 / (p_1 + p_0)$, where the definitions for p_0 and p_1 are given in Eq.(15).

Sequentially going through each individual e , the values for the initial z_e^i and proposed z_e^p states are calculated. Table 1 shows that for the Bernoulli distribution:

1) For $z_e^p > z_e^i$: if $D_e^i = 1$ we simply set $D_e^p = 1$, otherwise we draw a random number from 0 to 1 and if it is less than $\frac{z_e^p - z_e^i}{1 - z_e^i}$ we set $D_e^p = 1$ else $D_e^p = 0$.

2) For $z_e^p \leq z_e^i$: if $D_e^i = 0$ we simply set $D_e^p = 0$, otherwise we draw a random number from 0 to 1 and if it is less than $1 - \frac{z_e^p}{z_e^i}$ we set $D_e^p = 0$ else $D_e^p = 1$.

Gibbs samplers for disease prevalence model

For the disease diagnostic test model it is possible to explicitly sample directly from the posterior when model parameters and latent variables are each considered separately.

Model parameters: Assuming a uniform prior, the following samples are sequentially drawn from beta distributions

$$\begin{aligned} p_D &\sim \text{Beta}(N^1 + 1, N^0 + 1), \\ Se_1 &\sim \text{Beta}(N_1^{11} + 1, N_1^{01} + 1), \\ Sp_1 &\sim \text{Beta}(N_1^{00} + 1, N_1^{10} + 1), \\ Se_2 &\sim \text{Beta}(N_2^{11} + 1, N_2^{01} + 1), \\ Sp_2 &\sim \text{Beta}(N_2^{00} + 1, N_2^{10} + 1). \end{aligned} \quad (17)$$

Latent variables: Each individual e is considered in turn and, using the definitions in Eq.(15), we set $D_e=1$ with probability $p_1/(p_1+p_0)$ else $D_e=0$.

Appendix K: Details of the stochastic volatility model

In this appendix we provide additional details relevant to stochastic volatility model in Section 5.2.

Simulation and prior details

Simulated data was created using $\mu=-10$, $\phi=0.99$, $v=12$, $\sigma^2=0.0121$, and for simplicity the initial condition was set to $h_1=\mu$. Different value of correlation parameter ϕ were used to generate Fig. 8(b). The prior distributions for all variables were taken to be flat and in the ranges $-\infty-\infty$ for μ and h_1 , 0.001–0.999 for ϕ , 2–50 for v and 0– ∞ for σ^2 .

Observation model and latent process likelihood

We identify the following model parameters $\theta=\{\mu, \phi, v, \sigma^2, h_1\}$ and latent variables $\xi=\{h_{e>1}\}$. The DAG structure is illustrated in Fig. 7(a). The observation model and latent process likelihood are given by

$$\pi(y | \xi, \theta) = \prod_{e=1}^E \frac{\Gamma(\frac{\nu+1}{2})}{\sqrt{\nu\pi}\Gamma(\frac{\nu}{2})} \left(1 + \frac{y_e^2}{\nu e^{h_e}}\right)^{-\frac{\nu+1}{2}} e^{-h_e/2}, \quad (J1)$$

$$\pi(\xi | \theta) = \prod_{e=2}^E \frac{1}{\sqrt{2\pi\sigma^2}} e^{-\frac{(h_e - \mu - \phi(h_{e-1} - \mu))^2}{2\sigma^2}},$$

where Γ is the gamma function and E the observation period.

Importance distributions

ID₀ is given by the model

$$f_{ID_0}(h_e | h_{e' < e}, \theta) = f_{\text{norm}}(h_e | \mu_e^{\text{mod}}, \sigma^2), \quad (J2)$$

where $\mu_e^{\text{mod}} = \mu + \phi(h_{e-1} - \mu)$.

Equation (16) shows the expression for ID₁. The first thing to note is that the product of the model $\pi(\xi_e | \xi_{e' < e}, \theta)$ and observation probability $\pi(y_e | \xi_e, \theta)$ distributions from Eq.(J1) is not a standard distribution with which PBPs can be used (*i.e.* it is not listed in Table 1). One way around this problem is to first approximate the observation model as a normal distribution. This is achieved by Taylor series expanding $\log(\pi(y_e | \xi_e, \theta))$ about μ_e^{mod} up to second order, leading to

$$\pi(y_e | \xi_e, \theta) \cong f_{\text{norm}}(h_e | \mu_e^{\text{obs}}, \sigma_e^{\text{obs}2}), \quad (J3)$$

where

$$\mu_e^{\text{obs}} = \mu_e^{\text{mod}} + \frac{1}{2} \sigma_e^{\text{obs}2} \frac{\nu - q_e}{q_e + 1}, \quad \sigma_e^{\text{obs}2} = \frac{2(q_e + 1)^2}{q_e(\nu_e + 1)}, \quad q_e = \frac{\nu e^{\mu_e^{\text{mod}}}}{y_e^2}. \quad (J4)$$

The product of the two normal distributions in Eqs.(J2) and (J3) give

$$f_{ID_1}(h_e | h_{e' < e}, \theta, y) = f_{\text{norm}}(h_e | \frac{\mu_e^{\text{obs}} \sigma_e^2 + \mu_e^{\text{mod}} \sigma_e^{\text{obs}2}}{\sigma_e^{\text{obs}2} + \sigma^2}, \frac{\sigma_e^{\text{obs}2} \sigma^2}{\sigma_e^{\text{obs}2} + \sigma^2}). \quad (J5)$$

The definition of ID₂ from Eq.(17) is given by

$$f_{ID_2}(h_e | h_{e' < e}, \theta, y) \propto \pi(h_e | h_{e-1}, \theta) \pi(y_e | h_e, \theta) \int \pi(h_{e+1} | h_e, \theta) \pi(y_{e+1} | h_{e+1}, \theta) dh_{e+1}. \quad (J6)$$

In other words, the posterior distribution for h_e at time e depends not only on the value of h_{e-1} (*i.e.* the previous time point), but also on the observations at times e and $e+1$. In the general case this integral is intractable, but again following the Taylor series expansion approximation to the observation likelihood around $\bar{\mu} = \mu_e^{\text{mod}} = \mu + \phi(h_{e-1} - \mu)$, the following set of approximations can be made:

$$\begin{aligned}
\pi(h_e | h_{e-1}, \theta) &= f_{\text{norm}}(h_e | \bar{\mu}, \sigma^2), \\
\pi(y_e | h_e, \theta) &\cong f_{\text{norm}}(h_e | \mu_e^{\text{obs}}, \sigma_e^{\text{obs}2}), \\
\pi(h_{e+1} | h_e, \theta) &= f_{\text{norm}}(h_{e+1} | \mu + \phi(h_e - \mu), \sigma^2), \\
\pi(y_{e+1} | h_{e+1}, \theta) &\cong f_{\text{norm}}(h_{e+1} | \mu_{e+1}^{\text{obs}}, \sigma_{e+1}^{\text{obs}2}).
\end{aligned} \tag{J7}$$

where

$$\begin{aligned}
\mu_e^{\text{obs}} &= \bar{\mu} + \frac{1}{2} \sigma_e^{\text{obs}2} \frac{v - q_e}{q_e + 1}, \quad \sigma_e^{\text{obs}2} = \frac{2(q_e + 1)^2}{q_e(v_e + 1)}, \quad q_e = \frac{ve^{\bar{\mu}}}{y_e^2}, \\
\mu_{e+1}^{\text{obs}} &= \bar{\mu} + \frac{1}{2} \sigma_{e+1}^{\text{obs}2} \frac{v - q_{e+1}}{q_{e+1} + 1}, \quad \sigma_{e+1}^{\text{obs}2} = \frac{2(q_{e+1} + 1)^2}{q_e(v_{e+1} + 1)}, \quad q_{e+1} = \frac{ve^{\bar{\mu}}}{y_{e+1}^2}.
\end{aligned} \tag{J8}$$

Substituting the results from Eq.(J7) into (J6) gives

$$\begin{aligned}
f_{ID_2}(h_e | h_{e' < e}, \theta, y) &\propto f_{\text{norm}}(h_e | \bar{\mu}, \sigma^2) f_{\text{norm}}(h_e | \mu_e^{\text{obs}}, \sigma_e^{\text{obs}2}) \times \\
&\int f_{\text{norm}}(h_{e+1} | \mu + \phi(h_e - \mu), \sigma^2) f_{\text{norm}}(h_{e+1} | \mu_{e+1}^{\text{obs}}, \sigma_{e+1}^{\text{obs}2}) dh_{e+1}.
\end{aligned} \tag{J9}$$

Integrating over two normally distributed quantities is Gaussian distributed with respect to the difference in means with variance given by the sum of the variances of the two original distributions. Consequently, Eq.(J9) becomes

$$f_{ID_2}(h_e | h_{e' < e}, \theta, y) \propto f_{\text{norm}}(h_e | \bar{\mu}, \sigma^2) f_{\text{norm}}(h_e | \mu_e^{\text{obs}}, \sigma_e^{\text{obs}2}) \times e^{-\frac{(\mu + \phi(h_e - \mu) - \mu_{e+1}^{\text{obs}})^2}{2(\sigma^2 + \sigma_{e+1}^{\text{obs}2})}}. \tag{J10}$$

When written in terms of h_e the last term becomes another normal distribution

$$f_{ID_2}(h_e | h_{e' < e}, \theta, y) \propto f_{\text{norm}}(h_e | \bar{\mu}, \sigma^2) f_{\text{norm}}(h_e | \mu_e^{\text{obs}}, \sigma_e^{\text{obs}2}) f_{\text{norm}}(h_e | \mu_e^{\text{next}}, \sigma_e^{\text{next}2}), \tag{J11}$$

with mean and variance that capture information from the next observation (*i.e.* at time $e+1$)

$$\mu_e^{\text{next}} = \mu + \frac{\mu_{e+1}^{\text{obs}} - \mu}{\phi}, \quad \sigma_e^{\text{next}2} = \frac{\sigma^2 + \sigma_{e+1}^{\text{obs}2}}{\phi^2}. \tag{J12}$$

The product of the three normal distributions in Eq.(J11) gives the final result

$$f_{ID_2}(h_e | h_{e' < e}, \theta, y) = f_{\text{norm}}(h_e | \mu_e^{\text{res}}, \sigma_e^{\text{res}2}), \tag{J13}$$

where

$$\frac{1}{\sigma_e^{\text{res}2}} = \frac{1}{\sigma^2} + \frac{1}{\sigma_e^{\text{obs}2}} + \frac{1}{\sigma_e^{\text{next}2}}, \quad \frac{\mu_e^{\text{res}}}{\sigma_e^{\text{res}2}} = \frac{\bar{\mu}}{\sigma^2} + \frac{\mu_e^{\text{obs}}}{\sigma_e^{\text{obs}2}} + \frac{\mu_e^{\text{next}}}{\sigma_e^{\text{next}2}}. \tag{J14}$$

The standard approach for the stochastic volatility model

By multiplying the two expressions in Eq.(J1), the posterior distribution is given by

$$\pi(\mu, \phi, \nu, \sigma^2, \mathbf{h} | y) \propto \prod_{e=2}^E \frac{1}{\sqrt{2\pi\sigma^2}} e^{-\frac{(h_e - \mu - \phi(h_{e-1} - \mu))^2}{2\sigma^2}} \times \prod_{e=1}^E \frac{\Gamma(\frac{\nu+1}{2})}{\sqrt{\nu\pi}\Gamma(\frac{\nu}{2})} \left(1 + \frac{y_e^2}{\nu e^{h_e}}\right)^{-\frac{\nu+1}{2}} e^{-h_e/2}. \quad (\text{J15})$$

Rearranging this gives

$$\pi(\mu | y, \phi, \nu, \sigma^2, \mathbf{h}) \propto e^{-\frac{(1-\phi)^2(E-1)\left(\mu - \frac{1}{(1-\phi)(E-1)} \sum_{e=2}^E h_e - \phi h_{e-1}\right)^2}{2\sigma^2}}, \quad (\text{J16})$$

which takes the form of a standard normal distribution

$$\pi(\mu | y, \phi, \nu, \sigma^2, \mathbf{h}) = f_{\text{norm}}\left(\mu \mid \frac{1}{(1-\phi)(E-1)} \sum_{e=2}^E h_e - \phi h_{e-1}, \frac{\sigma^2}{(1-\phi)^2(E-1)}\right). \quad (\text{J17})$$

Consequently, μ is sampled in the following way:

$$\mu \sim N\left(\frac{1}{(1-\phi)(E-1)} \sum_{e=2}^E h_e - \phi h_{e-1}, \frac{\sigma^2}{(1-\phi)^2(E-1)}\right). \quad (\text{J18})$$

Similarly, the correlation parameter ϕ is also sampled from a normal distribution

$$\phi \sim N\left(\frac{\sum_{e=2}^E (h_e - \mu)(h_{e-1} - \mu)}{\sum_{e=2}^E (h_{e-1} - \mu)^2}, \frac{\sigma^2}{\sum_{e=2}^E (h_{e-1} - \mu)^2}\right). \quad (\text{J19})$$

The expression in Eq.(J15) can be rearranged to give

$$\pi(\sigma^2 | y, \mu, \phi, \nu, \mathbf{h}) \propto \frac{1}{\sigma^{E-1}} e^{-\frac{\sum_{e=2}^E (h_e - \mu - \phi(h_{e-1} - \mu))^2}{2\sigma^2}}, \quad (\text{J20})$$

which is an inverted chi-squared distribution with respect to σ^2 . All samples generated which have zero prior probability are subsequently resampled.

We adopt a simple random walk Metropolis-Hastings scheme (*i.e.* propose a new parameter / variable by adding a normally distributed contribution to its existing value and accepting or rejecting that change) for ν and h_e . In the case of h_e care is taken to only calculate those parts of the latent process likelihood and observation probability that actually change (to optimise the code as far as possible). The jumping sizes of the separate proposals are individually tuned to give acceptance approximately 33% of the time (using the same procedure as for j in Appendix C).

Appendix L: Details for mixed models

In this appendix we provide additional details relevant to the mixed models in Section 5.3.

Simulation and prior details

We introduce toy examples illustrating potential uses of MM in different contexts. In all cases flat uninformative priors were assumed for parameters.

Uncorrelated random effects: For this example we imagine that y represents test scores for pupils and the model contains two fixed effects: β_1 represents an average female score and β_2 gives the average difference in score between males and females (correspondingly, $X_{i1}=1$ and $X_{i2}=1/0$ depending on whether pupil i is male/female). Furthermore, we assume that the pupil's school is a random effect to take into account the fact that some schools are better than others, *i.e.* its value is drawn from a distribution with unknown variance σ_a^2 (correspondingly, $Z_{ie}=1$ if pupil i attends school e , otherwise $Z_{ie}=0$). Each a_e represents the random effect for school e and the measurements y_i represent the school's pupils. Because the random effects are uncorrelated (*i.e.* the quality of one school is not expected to affect the quality of another) so $A=I$. This scenario corresponds to the case in which the black solid lines in Fig. 9 (indicating dependences between random effects) are absent and each observations y_i is made on only a single random effect.

We simulate data assuming $E=100$ schools, $N=10000$ pupils randomly allocated to schools, gender randomly selected to be male or female (*i.e.* $X_{i2}=0$ or 1 with equal probability), $\beta=\{50,0.1\}$ and arbitrarily set the variance of the observations to be one, *i.e.* $\sigma_a^2 + \sigma_\varepsilon^2 = 1$.

Correlated random effects (A^{-1} sparse): Here we take y to represent measurements of height within a population. Two fixed effects are assumed: β_1 represents the average height of females and β_2 gives the average height difference between males and females. As illustrated in Fig. L1, here the model assumes a population of size P randomly mated over four generations (which leads to a sparse inverse matrix A^{-1} ²²). Here individuals in the 1st generation are

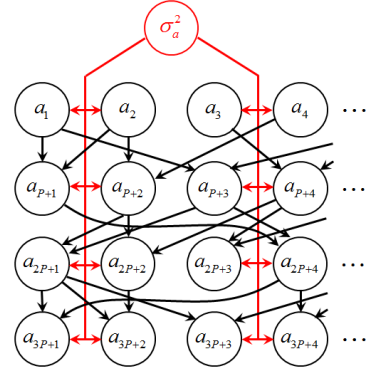


Figure L1: A specific quantitative genetics example in which a represent additive genetic effects for a population of P individuals randomly mated over four generations (note, for clarity β , and y have been omitted from this diagram). Note, for the non-founding population the random effect for each individual has contributions from its two parents in the previous generation.

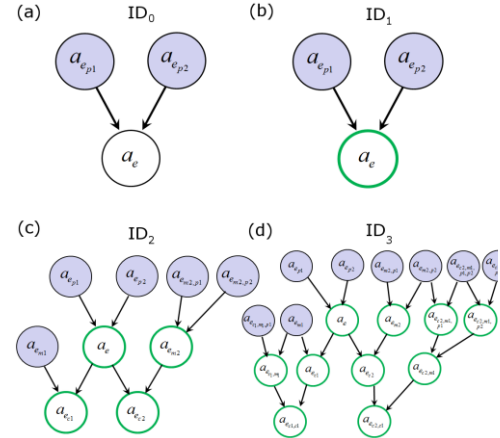


Figure L2: Various levels of approximation used for estimating $f_{ID}(a_e | a_{e' < e}, \theta, y)$ for the quantitative genetics model. The shaded circles represent known additive genetic effect $a_{e' < e}$ and the bold, green circles indicate the actual trait measurement used.

²² Individuals are related to themselves through $A_{nn}=1$ (assuming they are not inbred). If individual n is the parent of p then $A_{np}=1/2$, for siblings sharing the same parents $A_{np}=1/2$, for half-sibs $A_{np}=1/4$ and for a grandparent/grandchild relationship $A_{np}=1/4$ etc... Whilst A itself is not sparse, its inverse A^{-1} is (only diagonal and parent-sibling elements are non-zero).

assumed to be unrelated (*i.e.* conditionally independent) and those in the 2nd, 3rd and 4th generations are conditionally dependent on exactly two individuals in the previous generation (*i.e.* their parents). Simulated data was generated using a population size of $P=1000$, two fixed effects $\beta=\{1,0.1\}$, randomly allocated gender (*i.e.* $X_{i2}=0$ or 1 with equal probability along with $X_{i1}=1$) and one additive genetic effect per individual (*i.e.* $\mathbf{Z}=\mathbf{I}$).

Correlated random effects (\mathbf{A}^{-1} dense): Simulated data were generated in the same way as in the sparse case except that a small noise (uniformly sampled in the range between -0.005 and 0.005) was added to each element in \mathbf{A}^{-1} to mimic a typical genomic relationship matrix.

Observation model and latent process likelihood

We identify model parameters $\theta = \{\sigma_a^2, \sigma_e^2, \beta\}$ and latent variables $\xi = \{\mathbf{a}\}$, with residuals ε incorporated into the observation model.

At first glance it might appear that PBPs are not applicable to this particular model because the latent variables are MVN distributed (*i.e.* a distribution not contained within Table 1). This, however, turns out not to be the case, because of the following transformation.

The latent process likelihood is given by

$$\pi(\xi | \theta) = \pi(\mathbf{a} | \sigma_a^2) = \frac{1}{\sqrt{(2\pi\sigma_a^2)^E |\mathbf{A}|}} e^{-\frac{1}{2\sigma_a^2} \sum_{d=1}^E \sum_{e=1}^E a_d A_{de}^{-1} a_e}. \quad (\text{K1})$$

Separating out those terms which depend on a_E in the sum (and remembering that \mathbf{A} is symmetric and fixed), leads to the product of a normal distribution for a_E (given $a_{e' < E}$) multiplied by a new MVN distribution over the remaining $E-1$ latent variables

$$\pi(\mathbf{a} | \sigma_a^2) \propto f_{\text{norm}}(a_E | -\sum_{e'=1}^{E-1} A_{Ee'}^{-1} a_{e'}, \sigma_a^2 / A_{EE}^{-1}) \times \sigma_a^{-(E-1)} e^{-\frac{1}{2\sigma_a^2} \left(\sum_{d=1}^{E-1} \sum_{e=1}^{E-1} a_d (A_{de}^{-1} - A_{Ed}^{-1} A_{Ee}^{-1} / A_{EE}^{-1}) a_e \right)}, \quad (\text{K2})$$

where the p.d.f. for the univariate normal distribution is given by

$$f_{\text{norm}}(x | \mu, \sigma^2) = \frac{1}{\sqrt{2\pi\sigma^2}} e^{-\frac{(x-\mu)^2}{2\sigma^2}}. \quad (\text{K3})$$

The scheme above can be iterated until the original MVN distribution is converted into a product of normal distributions for each of the random effects

$$\pi(\mathbf{a} | \sigma_a^2) \propto \prod_{e=1}^E f_{\text{norm}}(a_e | \mu_e^{\text{mod}}, \sigma_e^{\text{mod}2}), \quad (\text{K4})$$

where

$$\mu_e^{\text{mod}} = \sum_{e' < e} M_{ee'} a_{e'}, \quad \sigma_e^{\text{mod}2} = s_e \sigma_a^2, \quad (\text{K5})$$

and matrix \mathbf{M} and vector \mathbf{s} are fixed and calculated from \mathbf{A} by recursively applying Eq.(K2). Note, Equation (K4) follows the same structure as Eq.(2), showing that it represents a DAG (specifically, the one illustrated in Fig. 9).

Under the above transformation, the observation model and latent process likelihood are given by

$$\begin{aligned}\pi(y | \xi, \theta) &= \prod_{i=1}^N f_{\text{norm}}(y_i | \sum_{f=1}^F X_{if} \beta_f + \sum_{e=1}^E Z_{ie} a_e, \sigma_\varepsilon^2), \\ \pi(\xi | \theta) &= f_{MVN}(\mathbf{a} | \mathbf{0}, \sigma_a^2 \mathbf{A}) \\ &\propto \prod_{e=1}^E f_{\text{norm}}(a_e | \mu_e^{\text{mod}}, \sigma_e^{\text{mod}2}),\end{aligned}\tag{K6}$$

where i goes over the observations, f goes over the fixed effects and e goes over the random effects.

Importance distributions

The different levels of ID approximation are illustrated in Fig. L2.

ID₀ is given by the model

$$f_{ID_0}(a_e | a_{e' < e}, \theta) = f_{\text{norm}}(a_e | \mu_e^{\text{mod}}, \sigma_e^{\text{mod}2}).$$

From Eq.(16), we see that ID₁ is generated by taking the product of the model and the observation probability distributions. For simplicity we assume that each observation contains a single random effect, but that each random effect may have many observations made on it (PBPs can also be applied in the more general case, but estimation of the IDs becomes somewhat more complicated).

A rearrangement of the observation model in Eq.(K4) leads to an effective observation probability for each individual random effect of

$$\pi(y_e | a_e, \theta) = f_{\text{norm}}(a_e | \mu_e^{\text{obs}}, \sigma_e^{\text{obs}2}),\tag{K7}$$

where y_e combines all observations y_i that include random effect a_e , and

$$\mu_e^{\text{obs}} = \frac{\sum_i (y_i - \sum_f X_{if} \beta_f) Z_{ie}}{\sum_i Z_{ie}^2}, \quad \sigma_e^{\text{obs}2} = \frac{\sigma_\varepsilon^2}{\sum_i Z_{ie}^2}.\tag{K8}$$

Taking the product of the two normal distributions in Eqs.(K4) and (K7) leads to the final result

$$f_{ID_1}(a_e | a_{e' < e}, \theta, y) = f_{\text{norm}}(a_e | \frac{\mu_e^{\text{obs}} \sigma_e^{\text{mod}2} + \mu_e^{\text{mod}} \sigma_e^{\text{obs}2}}{\sigma_e^{\text{obs}2} + \sigma_e^{\text{mod}2}}, \frac{\sigma_e^{\text{obs}2} \sigma_e^{\text{mod}2}}{\sigma_e^{\text{obs}2} + \sigma_e^{\text{mod}2}}).\tag{K9}$$

The distribution for ID₂ takes into account those random effects which depend on a_e . As stated in Eq.(17) and illustrated in Fig. 4(d), derivation of ID₂ involves integrating over those random effects a_d which depend on a_e . Explicitly writing down the expression for $f_{ID_2}(\xi_e | \xi_{e' < e}, \theta, y)$ is somewhat verbose. Instead, here we build up the final result by considering different contributions in turn.

To start with we consider a particular random effect a_d (which depends on a_e), and find out how it affects f_{ID_2} when it is integrated out. The contribution to the model part of the full posterior from a_d is given by

$$f_{norm}(a_d | \sum_{e'} M_{de'} a_{e'}, \sigma_d^{\text{mod}2}), \quad (\text{K10})$$

where e' sums over all those random effects on which a_d depends. Three possibility exist for e' : 1) $e' < e$, in which case $a_{e'}$ is known (as represented by the shaded circles in Fig. 4), 2) $e'=e$ and 3) $e' > e$, in which case the additional latent variable e' has to first be integrated out. In the case of the third option, Eq.(K10) is first recast in terms of the specific variable $e'=r$ that needs to be integrated out:

$$f_{norm}(a_r | \frac{a_d - \sum_{e' \neq r} M_{de'} a_{e'}}{M_{dr}}, \frac{\sigma_d^{\text{mod}2}}{M_{dr}^2}). \quad (\text{K11})$$

Now we remember that the posterior also has a contribution for a_r coming from its measurement and those random effects upon which it depends. These are captured by ID_1 from Eq.(K9), which is given by

$$f_{norm}(a_r | \mu_r^{\text{post}}, \sigma_r^{\text{post}2}), \quad (\text{K12})$$

where

$$\mu_r^{\text{post}} = \frac{\mu_r^{\text{obs}} \sigma_r^{\text{mod}2} + \mu_r^{\text{mod}} \sigma_r^{\text{obs}2}}{\sigma_r^{\text{obs}2} + \sigma_r^{\text{mod}2}}, \quad \sigma_r^{\text{post}2} = \frac{\sigma_r^{\text{obs}2} \sigma_r^{\text{mod}2}}{\sigma_r^{\text{obs}2} + \sigma_r^{\text{mod}2}}. \quad (\text{K13})$$

Multiplying Eqs.(K11) and (K12) and integrating over a_r leads to the posterior probability being proportional to

$$e^{-\frac{1}{2} \left(\frac{\sigma_d^{\text{mod}2}}{M_{dr}^2} + \sigma_r^{\text{post}2} \right) \left(\frac{a_d - \sum_{e' \neq r} M_{de'} a_{e'}}{M_{dr}} - \mu_r^{\text{post}} \right)^2}. \quad (\text{K14})$$

This can again be re-cast in terms of a_d :

$$f_{norm}(a_d | M_{dr} \mu_r^{\text{post}} + \sum_{e' \neq r} M_{de'} a_{e'}, \sigma_d^{\text{mod}2} + M_{dr}^2 \sigma_r^{\text{post}2}). \quad (\text{K15})$$

Compared to the original expression in Eq.(K10), we see that the effect of integrating out a_r is to replace a_r with the posterior estimate μ_r^{post} in the mean and to add an additional contribution to the variance. The procedure above can be repeated for all $e' > e$, leading to

$$f_{norm}(a_d | \sum_{e' < e} M_{de'} a_{e'} + M_{ee} a_e + \sum_{e' > e} M_{de'} \mu_{e'}^{\text{post}}, \sigma_d^{\text{mod}2} + \sum_{e' > e} M_{de'}^2 \sigma_{e'}^{\text{post}2}). \quad (\text{K16})$$

We now introduce the contribution which comes from the observation on a_d itself:

$$f_{norm}(a_d | \mu_d^{\text{obs}}, \sigma_d^{\text{obs}2}). \quad (\text{K17})$$

Multiplying Eqs.(K16) and (K17) and integrating over a_d implies that the posterior is proportional to

$$e^{-\frac{1}{2} \left(\sigma_d^{\text{mod}2} + \sigma_d^{\text{obs}2} + \sum_{e' > e} M_{de'}^2 \sigma_{e'}^{\text{post}2} \right) \left(\sum_{e' < e} M_{de'} a_{e'} + M_{ee} a_e + \sum_{e' > e} M_{de'} \mu_{e'}^{\text{post}} - \mu_d^{\text{obs}} \right)^2}. \quad (\text{K18})$$

This can be recast in terms of a_e :

$$f_{\text{norm}}(a_e | \mu_{d \rightarrow e}, \sigma_{d \rightarrow e}^2), \quad (\text{K19})$$

where

$$\begin{aligned} \mu_{d \rightarrow e} &= \frac{\mu_d^{\text{obs}} - \left(\sum_{e' < e} M_{de'} a_{e'} + \sum_{e' > e} M_{de'} \mu_{e'}^{\text{post}} \right)}{M_{ee}}, \\ \sigma_{d \rightarrow e}^2 &= \frac{\sigma_d^{\text{mod}2} + \sigma_d^{\text{obs}2} + \sum_{e' > e} M_{de'}^2 \sigma_{e'}^{\text{post}2}}{M_{ee}^2}. \end{aligned} \quad (\text{K20})$$

Equation (K19) represents the overall contribution to f_{ID2} from latent variable d . To find f_{ID2} , therefore, this distribution must be multiplied over all random effects d which depend on a_e , and also the observation and model contributions from a_e itself must be included:

$$f_{\text{norm}}(a_e | \mu_e^{\text{post}}, \sigma_e^{\text{post}2}) \prod_d f_{\text{norm}}(a_e | \mu_{d \rightarrow e}, \sigma_{d \rightarrow e}^2). \quad (\text{K21})$$

Multiplication of these normal distributions yield the final result

$$f_{ID_2}(a_e | a_{e' < e}, \theta, y) = f_{\text{norm}}(a_e | \mu_e^{ID}, \sigma_e^{ID2}), \quad (\text{K22})$$

where

$$\begin{aligned} \mu_e^{ID} &= \left(\frac{\mu_e^{\text{post}}}{\sigma_e^{\text{post}2}} + \sum_d \frac{\mu_{d \rightarrow e}}{\sigma_{d \rightarrow e}^2} \right) \sigma_e^{ID2}, \\ \frac{1}{\sigma_e^{ID2}} &= \frac{1}{\sigma_e^{\text{post}2}} + \sum_d \frac{1}{\sigma_{d \rightarrow e}^2}. \end{aligned} \quad (\text{K23})$$

The distribution for ID_{2a} is calculated in exactly the same way as for ID_2 except that only those contributions with $|M_{ee'}| > 0.1$ are included in the sum in Eq.(K5).

Gibbs samplers for mixed models

Mixed models represent a case for which it is possible to explicitly sample directly from the posterior when model parameters and latent variables are each considered separately [30]. Assuming a simple uniform prior²³, multiplying the two expressions in Eq.(K6) leads to the posterior probability distribution

$$\pi(\sigma_a^2, \sigma_\varepsilon^2, \boldsymbol{\beta}, \mathbf{a} | \mathbf{y}) \propto \frac{1}{\sqrt{(2\pi\sigma_a^2)^E |A|}} e^{-\frac{1}{2\sigma_a^2} \mathbf{a}^T A^{-1} \mathbf{a}} \prod_{i=1}^N \frac{1}{\sqrt{2\pi\sigma_\varepsilon^2}} e^{-\frac{1}{2\sigma_\varepsilon^2} \left(y_i - \sum_j X_{ij} \beta_j - \sum_e Z_{ie} a_e \right)^2}. \quad (\text{K24})$$

The following Gibbs proposals can be identified, which are sequentially applied to constitute a single “update”:

Model parameters: Rearranging (K24) gives

²³ Non-uniform priors can be easily be implemented provided they also take an inverted chi-squared distribution.

$$\pi(\sigma_a^2 | \mathbf{y}, \sigma_\varepsilon^2, \boldsymbol{\beta}, \mathbf{a}) \propto \sigma_a^{-E} e^{-\frac{1}{2\sigma_a^2} \mathbf{a}^T \mathbf{A}^{-1} \mathbf{a}}. \quad (\text{K25})$$

That is, with all other quantities fixed the posterior has an inverted chi-squared distribution with respect to σ_a^2 . Similarly, we find that

$$\pi(\sigma_\varepsilon^2 | \mathbf{y}, \sigma_a^2, \boldsymbol{\beta}, \mathbf{a}) \propto \sigma_\varepsilon^{-N} e^{-\frac{1}{2\sigma_\varepsilon^2} \sum_{i=1}^N (y_i - \sum_f X_{if} \beta_f - \sum_e Z_{ie} a_e)^2}, \quad (\text{K26})$$

and so σ_ε^2 also has an inverted chi-squared distribution. See below for how to draw samples from the inverted chi-squared distributions in Eqs.(K25) and (K26).

Taking each fixed effect β_f in turn, the posterior can be written as

$$\pi(\beta_f | \mathbf{y}, \sigma_a^2, \sigma_\varepsilon^2, \boldsymbol{\beta}_{f' \neq f}, \mathbf{a}) = f_{\text{norm}} \left(\beta_f | \sum_i X_{if} \left[y_i - \sum_{f' \neq f} X_{if'} \beta_{f'} - \sum_e Z_{ie} a_e \right], \frac{\sigma_\varepsilon^2}{\sum_i X_{if}^2} \right). \quad (\text{K27})$$

Thus, its value can be sampled from the following normal distribution

$$\beta_f \sim N \left(\sum_i X_{if} \left[y_i - \sum_{f' \neq f} X_{if'} \beta_{f'} - \sum_e Z_{ie} a_e \right], \frac{\sigma_\varepsilon^2}{\sum_i X_{if}^2} \right). \quad (\text{K28})$$

Latent variables: Gibbs sampling for random effect a_e is achieved through

$$a_e \sim N \left(\mu_e^{\text{gibbs}}, \sigma_e^{\text{gibbs}2} \right), \quad (\text{K29})$$

where

$$\begin{aligned} \mu_e^{\text{gibbs}} &= \left(\frac{1}{\sigma_\varepsilon^2} \sum_i Z_{ie} \left[y_i - \sum_f X_{if} \beta_f - \sum_{e' \neq e} Z_{ie'} a_{e'} \right] - \frac{1}{\sigma_a^2} \sum_{e' \neq e} A_{ee'}^{-1} a_{e'} \right), \\ \frac{1}{\sigma_e^{\text{gibbs}2}} &= \frac{1}{\sigma_a^2} + \frac{\sum_i Z_{ie}^2}{\sigma_\varepsilon^2}. \end{aligned} \quad (\text{K30})$$

Sampling from the inverse chi-squared distribution

We assume an inverse chi-squared distribution of the form

$$f_\chi(x | N, S) \propto x^{-\frac{M}{2}} e^{-\frac{S}{2x}}. \quad (\text{K31})$$

A simple method to calculate samples from this distribution is through

$$x = \frac{S}{2\rho}, \quad \rho = -\sum_{m=1}^{M-1} \log(u_m), \quad (\text{K32})$$

where u_m are uniform randomly generated numbers between 0 and 1.

Appendix M: Details for the generalized linear mixed model

In this appendix we provide additional details relevant to the generalized linear mixed model in Section 5.4.

Simulation and prior details

Simulations were performed assuming a population of $P=1000$ individuals randomly mated over four generations with two fixed effects: β_1 represents the average propensity to disease for females and β_2 gives the difference in propensity between males and females. Various values for σ_a^2 were used to generate the results in Fig. 11. Values for the fixed effects were $\beta=\{1,0.1\}$, and gender of individuals was randomly allocated (*i.e.* $X_{i2}=0$ or 1 with equal probability along with $X_{i1}=1$).

Observation model and latent process likelihood

For this GLMM model we identify model parameters $\theta = \{\sigma_a^2, \beta\}$ and latent variables $\xi = \{a\}$. The observation model and latent process likelihood (which can be represented by a DAG using the procedure outlined in Appendix L) are given by

$$\begin{aligned} \pi(y | \xi, \theta) &= \prod_{e=1}^E \frac{1}{1 + e^{-S_e(\sum_f X_{ef} \beta_f + a_e)}}, \\ \pi(\xi | \theta) &\propto \prod_{e=1}^E f_{\text{norm}}(a_e | \mu_e^{\text{mod}}, \sigma_e^{\text{mod}2}), \end{aligned} \quad (\text{L1})$$

where μ_e^{mod} and $\sigma_e^{\text{mod}2}$ are defined in Eq.(K5) and the sign $S_e=1$ or -1 correspond to whether the disease status for individual e is 1 or 0, respectively.

Importance distributions

ID_0 is given by the latent process model:

$$f_{ID_0}(a_e | a_{e' < e}, \theta) = f_{\text{norm}}(a_e | \mu_e^{\text{mod}}, \sigma_e^{\text{mod}2}). \quad (\text{L2})$$

To generate ID_1 first the observation model is approximated by a normal distribution (this is achieved by Taylor series expanding the log of the observation probability about μ_e^{mod} up to second order)

$$\pi(y_e | a_e, \theta) \cong f_{\text{norm}}(a_e | \mu_e^{\text{obs}}, \sigma_e^{\text{obs}2}), \quad (\text{L3})$$

where

$$\mu_e^{\text{obs}} = \mu_e^{\text{mod}} + S_e \frac{q+1}{q}, \quad \sigma_e^{\text{obs}2} = \frac{(q+1)^2}{q}, \quad q = e^{S_e(\sum_f X_{ef} \beta_f + \mu_e^{\text{mod}})}. \quad (\text{L4})$$

From Eq.(21), ID_1 is found by taking the product of ID_0 in Eq.(L2) and the observation probability at the current latent variable in Eq.(L3). This leads to the final result

$$f_{ID_1}(a_e | a_{e' < e}, \theta, y) = f_{\text{norm}}\left(a_e \mid \frac{\mu_e^{\text{obs}} \sigma_e^{\text{mod}2} + \mu_e^{\text{mod}} \sigma_e^{\text{obs}2}}{\sigma_e^{\text{obs}2} + \sigma_e^{\text{mod}2}}, \frac{\sigma_e^{\text{obs}2} \sigma_e^{\text{mod}2}}{\sigma_e^{\text{obs}2} + \sigma_e^{\text{mod}2}}\right). \quad (\text{L5})$$

The standard approach for the binary GLMM

In the case of GLMMs Gibbs sampling is not possible due to the posterior no longer having a standard form when marginalised in the various parameters and variables (with the exception of σ_a^2 , which can still be sampled from an inverse chi-squared distribution). Consequently we adopt a simple random walk Metropolis-Hastings scheme (*i.e.* we propose a new parameter / variable by adding a normally distributed contribution to its existing value and accepting or rejecting that change). The jumping sizes of the separate proposals are individually tuned to give acceptance approximately 33% of the time (achieved using the same adaptation procedure for j in Appendix C).

References

- [1] W. R. Gilks, S. Richardson, and D. J. Spiegelhalter, *Markov chain Monte Carlo in practice*. Boca Raton, Fla.: Chapman & Hall, 1998.
- [2] S. Brooks, A. Gelman, G. Jones, and X.-L. Meng, *Handbook of markov chain monte carlo*: CRC press, 2011.
- [3] C. Andrieu, A. Doucet, and R. Holenstein, "Particle Markov chain Monte Carlo methods," *J. R. Stat. Soc. B*, vol. 72, pp. 269-342, 2010.
- [4] R. M. Neal, "MCMC Using Hamiltonian Dynamics," *Handbook of Markov Chain Monte Carlo*, pp. 113-162, 2011.
- [5] O. Papaspiliopoulos, G. O. Roberts, and M. Skold, "Non-centered parameterisations for hierarchical models and data augmentation," in *Bayesian Statistics 7*, 2003, pp. 307-326.
- [6] N. Friel and J. Wyse, "Estimating the evidence – a review," *Statistica Neerlandica*, vol. 66, pp. 288-308, 2012.
- [7] W. K. Hastings, "Monte-Carlo Sampling Methods Using Markov Chains and Their Applications," *Biometrika*, vol. 57, p. 97, 1970.
- [8] G. Casella and E. I. George, "Explaining the Gibbs Sampler," *The American Statistician*, vol. 46, pp. 167-174, 1992.
- [9] R. M. Neal, "Slice sampling," *Annals of Statistics*, vol. 31, pp. 705-741, Jun 2003.
- [10] C. M. Pooley, S. C. Bishop, and G. Marion, "Using model-based proposals for fast parameter inference on discrete state space, continuous-time Markov processes," *Journal of the Royal Society Interface*, vol. 12, 2015.
- [11] K. Csilléry, M. G. Blum, O. E. Gaggiotti, and O. François, "Approximate Bayesian computation (ABC) in practice," *Trends in Ecology & Evolution*, vol. 25, pp. 410-418, 2010.
- [12] C. P. Robert, J.-M. Cornuet, J.-M. Marin, and N. S. Pillai, "Lack of confidence in approximate Bayesian computation model choice," *Proceedings of the National Academy of Sciences*, vol. 108, pp. 15112-15117, 2011.
- [13] M. D. Hoffman and A. Gelman, "The No-U-turn sampler: adaptively setting path lengths in Hamiltonian Monte Carlo," *Journal of Machine Learning Research*, vol. 15, pp. 1593-1623, 2014.
- [14] M. J. Keeling and P. Rohani, *Modeling infectious diseases in humans and animals*. Princeton: Princeton University Press, 2008.
- [15] G. J. Gibson and E. Renshaw, "Estimating parameters in stochastic compartmental models using Markov chain methods," *Ima. J. Math Appl. Med.*, vol. 15, pp. 19-40, Mar 1998.
- [16] P. Neal and G. Roberts, "A case study in non-centering for data augmentation: Stochastic epidemics," *Stat. Comput.*, vol. 15, pp. 315-327, 2005.
- [17] O. Papaspiliopoulos, G. O. Roberts, and M. Skold, "A general framework for the parametrization of hierarchical models," *Statistical Science*, vol. 22, pp. 59-73, Feb 2007.

- [18] K. Thulasiraman and M. N. S. Swamy, "Directed Graphs," in *Graphs: Theory and Algorithms*, ed: John Wiley & Sons, Inc., 1992, pp. 97-125.
- [19] M. Lynch and B. Walsh, *Genetics and analysis of quantitative traits* vol. 1: Sinauer Sunderland, MA, 1998.
- [20] W. W. Stroup, *Generalized linear mixed models: modern concepts, methods and applications*: CRC press, 2012.
- [21] S. Karlin, *A first course in stochastic processes*: Academic press, 2014.
- [22] J. L. McDonald, A. Robertson, and M. J. Silk, "Wildlife disease ecology from the individual to the population: Insights from a long-term study of a naturally infected European badger population," *Journal of Animal Ecology*, vol. 87, pp. 101-112, 2018.
- [23] S. Chib, F. Nardari, and N. Shephard, "Markov chain Monte Carlo methods for stochastic volatility models," *Journal of Econometrics*, vol. 108, pp. 281-316, 2002.
- [24] N. Hautsch and Y. Ou, "Discrete-time stochastic volatility models and MCMC-based statistical inference," 2008.
- [25] R. A. Mclean, W. L. Sanders, and W. W. Stroup, "A Unified Approach to Mixed Linear-Models," *American Statistician*, vol. 45, pp. 54-64, Feb 1991.
- [26] R. A. Fisher, "XV.—The correlation between relatives on the supposition of Mendelian inheritance," *Earth and Environmental Science Transactions of the Royal Society of Edinburgh*, vol. 52, pp. 399-433, 1919.
- [27] B. Baltagi, *Econometric analysis of panel data*: John Wiley & Sons, 2008.
- [28] N. M. Laird and J. H. Ware, "Random-effects models for longitudinal data," *Biometrics*, vol. 38, pp. 963-974, 1982.
- [29] T. Koerner and Y. Zhang, "Application of linear mixed-effects models in human neuroscience research: a comparison with Pearson correlation in two auditory electrophysiology studies," *Brain sciences*, vol. 7, p. 26, 2017.
- [30] D. Sorensen and D. Gianola, *Likelihood, Bayesian and MCMC methods in quantitative genetics*. New York: Springer-Verlag, 2002.
- [31] M. E. Goddard, B. J. Hayes, and T. H. E. Meuwissen, "Using the genomic relationship matrix to predict the accuracy of genomic selection," *Journal of Animal Breeding and Genetics*, vol. 128, pp. 409-421, 2011.
- [32] K. Thulasiraman and M. N. Swamy, *Graphs: theory and algorithms*: John Wiley & Sons, 2011.
- [33] D. S. Falconer, *Introduction to quantitative genetics*: Oliver And Boyd; Edinburgh; London, 1960.
- [34] T. Price and D. Schluter, "On the low heritability of life-history traits," *Evolution*, vol. 45, pp. 853-861, 1991.
- [35] A. Doucet, N. De Freitas, and N. Gordon, "An introduction to sequential Monte Carlo methods," in *Sequential Monte Carlo methods in practice*, ed: Springer, 2001, pp. 3-14.
- [36] P. W. Glynn and D. L. Iglehart, "Importance sampling for stochastic simulations," *Management Science*, vol. 35, pp. 1367-1392, 1989.
- [37] C. Andrieu and J. Thoms, "A tutorial on adaptive MCMC," *Statistics and Computing*, vol. 18, pp. 343-373, 2008/12/01 2008.
- [38] G. O. Roberts and J. S. Rosenthal, "Examples of Adaptive MCMC," *Journal of Computational and Graphical Statistics*, vol. 18, pp. 349-367, 2009/01/01 2009.
- [39] W. H. Press, *FORTRAN numerical recipes*, 2nd ed. Cambridge England ; New York: Cambridge University Press, 1996.
- [40] C. J. Geyer, "Practical Markov Chain Monte Carlo," *Statist. Sci.*, vol. 7, pp. 473-483, 1992/11 1992.